

International Journal of Modern Physics E
 © World Scientific Publishing Company

**Deformed magic numbers at $N = 178$ and $Z = 120, 124$
 in the $112 \leq N \leq 190$ superheavy region
 from Skyrme mean-field calculations**

W. Asous

*Department of Applied Physics, Faculty of Science and Technology, Universiti Kebangsaan
 Malaysia (UKM), 43600 Bangi, Selangor, Malaysia.
 wissalasous@gmail.com*

Mastura Syamimi Abdullah

*Department of Physics, Faculty of Science, Universiti Teknologi Malaysia, 81310 Johor Bahru,
 Johor, Malaysia.*

Meng-Hock Koh*

*Department of Physics, Faculty of Science, Universiti Teknologi Malaysia, 81310 Johor Bahru,
 Johor, Malaysia.
 UTM Centre for Industrial and Applied Mathematics, Universiti Teknologi Malaysia, 81310
 Johor Bahru, Johor, Malaysia.
 kmhock@utm.my*

Kok-Siong Khoo

*Department of Applied Physics, Faculty of Science and Technology, Universiti Kebangsaan
 Malaysia (UKM), 43600 Bangi, Selangor, Malaysia.
 Nuclear Technology Research Centre (NUKLEAR), Faculty of Science and Technology,
 Universiti Kebangsaan Malaysia 43600 Bangi. Selangor Malaysia.*

Received Day Month Year

Revised Day Month Year

Background: Various motivations for exploration of superheavy region revolve around the question on whether 126 is a spherical proton magic number, as is the case for neutrons. In exploring this region, identification of nuclei with relatively longer half-life as compared to its neighbours is crucial for experimental studies. Such information are provided from theoretical predictions, which are however, heavily dependent on the theoretical model used and observable quantities under investigation.

Purpose: Limiting ourselves to the Skyrme Hartree-Fock-plus-Bardeen-Cooper-Schrieffer approach, we aimed to analyse the appearance of a nuclear region with relatively high stability associated with emergence of spherical and deformed magic numbers in the region of $170 \leq N \leq 190$ ($112 \leq Z \leq 130$) based on various observables.

Methods: Three Skyrme parametrizations namely the SkM* frequently employed for

*kmhock@utm.my

fission calculations, and the SLy5 and SLy4 commonly used for superheavy region, are considered to provide comparisons within the Skyrme mean-field approach. We evaluated the variation of electric quadrupole deformation (β_{20}), binding energy per nucleon (BE/A), two-nucleon separation energy differential (δS_{2q}), alpha-decay energy (Q_α) and alpha-decay half-lives ($T_{1/2}$).

Conclusion: Our analyses suggest that neutron number $N = 178$ is candidate for deformed magic number around proton number $114 \leq Z \leq 118$. For protons, $Z = 120$ and 124 appears to be a candidate for deformed magic number at around $N = 172 \sim 178$. Both sets of deformed magic numbers appear at oblate ground-state deformation.

Keywords: Hartree-Fock; superheavy nuclei; alpha-decay; Q_α , half lives, magic numbers.

PACS numbers:

1. Introduction

Investigation of superheavy (SH) region with atomic number of $Z \geq 104$ is fuelled by the motivation to explore the limits of nuclear chart¹ at the upper right region. The heaviest element produced thus far is the Oganesson with atomic number (Z) = 118^{2–4}. The basis for exploring this superheavy region is that the 126 is expected to be magic for protons as was the case for neutrons.⁴ In practice, one would require making multiple stops before the $Z = 126$ can be synthesized. These stops refers to nuclei with specific combination of proton Z and neutron N numbers which have sufficiently long half-life as compared to its neighbouring nuclei. In this context, theoretical calculations to identify stable isotopes as compared to their neighbours would be handy as experimentalists explores the SH region.

However, theoretical predictions of nuclei with magic or sub-magic numbers are heavily model-dependent and often provide a conflicting results. On the one hand, there are the microscopic calculations based on the mean-field and beyond mean-field frameworks^{5–21}. On the other hand, there are the microscopic–macroscopic models for e.g. those based on the cluster decay^{22–29}, and generalized- and effective-liquid drop model^{30–32}. Alpha-decay models such as the Coulomb and proximity potential model and deformed nuclei (CPPM and CPPMDN) have also been used to explore the SHE region^{33–44}.

In all these studies, observable quantities of interest are indeed the alpha-decay namely Q_α -values and half-lives $T_{1/2}$ since nuclei in this region tends to decay via alpha emission. In addition, observables such as binding energy and two-nucleon separation differential (shell-gap) have also been considered for e.g. in the work of Refs.^{5,9}. Table 1 shows a non-exhaustive list of proton and neutron magic or sub-magic numbers obtained from these predictions.

For protons, we find that $Z = 114$ and 120 are often reproduced by most methods. In the case of neutrons, the predicted magic or sub-magic numbers are less certain with estimated range between $N = 172$ to $N = 178$. In addition to these sets of proton and neutron magic numbers, one should also include the spherical doubly magic nucleus with $Z = 126$ and $N = 184$.

It is the purpose of this work to revisit the investigation of magic and sub-

magic numbers through cross-analyses of quantities which are sensitive to shell effect namely two-nucleon separation energies and single-particle levels, and, bulk properties in the form of alpha-decay energy Q_α and half-life $T_{1/2}$. We have limit ourselves herein to nuclei in the region of $112 \leq Z \leq 130$ and $170 \leq N \leq 190$ which are expected to be relevant to the current experimental progress.

Our work relies on the Skyrme–Hartree–Fock–plus–Bardeen–Cooper–Schrieffer (SHF+BCS) framework which will be discussed in Section 2.1. Calculations of Q_α and half-lives $T_{1/2}$ using the binding energies obtained from the SHF+BCS are then discussed in Section 2.2. Section 3 will be dedicated to the analyses of ground-state deformation, separation energies differential, single-particle levels, and alpha-decay properties. Finally, conclusion of the work will be discussed in Section 4.

2. Theoretical Framework

2.1. The Skyrme mean-field model

The standard Skyrme HF+BCS model is used in our study. We considered primarily two Skyrme parametrizations namely the SkM*⁵³ and the SLy5⁵⁴. The SkM* parametrization was fitted in the early 1980s and has been commonly employed in nuclear fission study. As was the case for other parametrizations fitted in the early years of nuclear mean-field calculations, the spin-orbit density J term was neglected in the SkM* fit procedure. In contrast, the SLy5 parametrization fitted in the 1990s takes into account the spin-orbit density term. Apart from this difference, the fit procedures for both parametrizations are similar in that they use a density dependence of $\alpha = 1/6$ and the Coulomb exchange term is treated using the Slater approximation. It is also interesting to note that the SLy5 parametrization was found to suffer from spin-instability arising from the $s\Delta s$ term in the Skyrme energy density functional. The SLy5 parametrization was then refitted by⁵⁵ to overcome this issue leading to the new SLy5* parametrization.

In addition, we also compared the results with those obtained using the SLy4 parametrization which was reported to perform well in the superheavy region^{56, 57}.

For the particle-hole part, we employed the seniority force where the pairing matrix element is given by:

$$v_{k\bar{k}l\bar{l}} = \frac{G_q}{11 + N_q}, \quad (1)$$

with G_q and N_q being the pairing strength and total nucleon number of a given charge state $q \equiv \{n, p\}$.

The pairing strength G_q was initially fitted such that the BCS pairing gap reproduces the empirical Madland formula of each nucleus given by:

$$\Delta_n = r \exp\left(\frac{-sI - tI^2}{N^{1/3}}\right), \quad (2)$$

$$\Delta_p = r \exp\left(\frac{sI - tI^2}{Z^{1/3}}\right). \quad (3)$$

Table 1. Summary predictions of magic and sub-magic numbers through analyses of observable quantities based on the theoretical models of Hartree-Fock-plus-Bardeen–Cooper–Schrieffer (HF+BCS), Hartree-Fock-Bogoliubov (HFB), Effective Liquid-Drop-Model (ELDM), Generalized-Liquid-Drop-Model (GLDM), Weizsäcker–Skyrme 4 (WS4), Relativistic-Mean-Field (RMF), Density-Dependent Cluster-Model (DD-CM), Macroscopic-Microscopic (Mac-mic), Coulomb and Proximity Potential Model (CPPM) and for Deformed Nuclei (CPPMDN).

Model	Quantity	Z	N	Refs.
HF+BCS	δ_{2q}	114, 126	184	5
	SPS	114, 126	184	7
	SPS	120	172	7
	SC	124, 126	184	9
	Δ_q , S_{2n} , SPS	120	172, 182, 208	11
	SPS	164	308	12
HFB	SPS	120	172	45
	Shell-gap	120, 126	172, 184	10, 46
ELDM	Q_α , $T_{1/2}$	120	178, 184	32
GLDM	$T_{1/2}$	114	184	31
	$T_{1/2}$	120, 126	184	31
	Q_α , $T_{1/2}$		162, 178, 184	47
WS4	δ_{2q}	114	184	48
		120	178	48
RMF	δ_{2q} , SPS	120	172	5, 7
	SC	120	172	9
	SPS	120	172, 184	6
	BE/A , SPS	114	164 ~ 172	8
	BE/A , SPS	120	172, 184	8
	δ_{2n} , SPS	–	168, 174, 178	49
	δ_{2q} , SPS	120, 138	172, 184, 228, 258	13
	Δ_q , S_{2n} , SPS	120	172, 184, 258	11
DD-CM		82, 98	126, 148	
		100, 102	152, 154	
		106, 108	160, 162	
	$T_{1/2}$	114, 116	172, 176	27
			178, 180	
			180, 182	
			184, 200	
Mac-Mic	$T_{1/2}$	–	178	50
	SC	114, 120	174, 184	51, 52
CPPMDN	$T_{1/2}$	120	178	34
CPPM	$T_{1/2}$	–	184	33
	$T_{1/2}$	–	184, 202	41

Table 2. Averaged pairing strengths of SkM* and SLy5 Skyrme parametrizations taken from 86 nuclei whereby the pairing strengths for each nucleus have been fitted to the Madland pairing gap formula.

Skyrme type	$G_n^{Avg.}$ (MeV)	$G_p^{Avg.}$ (MeV)
SkM*	14.79	13.72
SLy5	16.72	14.25
SLy4	16.72	14.25

Table 3. Basis size test on Og-294 with SkM* and SLy5 Skyrme parametrization.

N_0	$Q_\alpha^{SkM^*}$ (MeV)	Q_α^{SLy5} (MeV)
14	11.86	11.66
16	12.18	11.74
18	12.17	11.40
20	12.20	11.43
22	12.22	11.41

The constants entering the formula are $r = 5.72$ MeV, $s = 0.118$ and $t = 8.12$ while $I = \frac{N-Z}{A}$ is the neutron excess.

Fitting G_q in such a manner may yield values which are artificially increased especially when the single-particle level density at the mean-field level is not correctly reproduced. We therefore took an average pairing strength for the neutron and proton channels separately, of the 86 superheavy nuclei considered herein. The retained values (in MeV) are shown in Table 2. The pairing strengths for the SLy4 parametrizations are taken to be the same as those of the SLy5 values.

The single-particle wave-function is expanded on the harmonic oscillator basis states and the expansion is truncated such that:

$$\hbar\omega_\perp(n_\perp + 1) + \hbar\omega_z(n_z + \frac{1}{2}) \leq \hbar\omega_0(N_0 + 2), \quad (4)$$

with the basis size of $N_0 = 18$. The spherical angular frequency $\omega_0^3 = \omega_\perp^2 \omega_z$ is related to the angular frequency ω_\perp in the $x - y$ plane and ω_z in the z -direction.

The basis size is selected through comparison on Q_α values as a function of N_0 in Og-294 isotope. These values are tabulated in Table 3. It can be seen that the Q_α remains almost constant after $N_0 = 16$ with the SkM* parametrization and after $N_0 = 18$ with the SLy5 parametrization. Therefore, we opt to retain $N_0 = 18$ for both forces.

The numerical integration is handled using Gauss-Hermite and Gauss-Laguerre approximations with 50 and 20 points, respectively. The exchange Coulomb term is calculated using the usual Slater approximation.⁵⁸ The ground-state is assumed

to be axially and parity symmetric shape.⁵⁹

2.2. Alpha-decay half-lives formulas

We use the absolute value of the binding energy (E_B) from the Skyrme mean-field model to calculate the Q_α using the expression:

$$Q_\alpha(Z, N) = E_B(2, 2) + E_B(Z - 2, N - 2) - E_B(Z, N), \quad (5)$$

where $E_B(2, 2) = 28.3$ MeV is the binding energy of He-4 nucleus. We consider only the case whereby the alpha decay occurs from the ground-state of parent nucleus to the ground-state of daughter nucleus. The value of Q_α enters the alpha decay half-life formulas as discussed in the following subsections.

2.2.1. Viola-Seaborg (VS) formula

The Viola-Seaborg formula⁶⁰ was developed based on the Gamow model with the half-life given by the expression:

$$\log_{10} T_{1/2}^{VS} = (aZ + b)Q^{-\frac{1}{2}} + cZ + d + h. \quad (6)$$

Over the years, the original parameters of⁶⁰ have been refitted as new experimental data emerged. We considered herein two sets of parameters to the Viola-Seaborg formula. The first is referred to as the VSS1 taken from the work of Sobiczewski and Cwiok⁶¹. The parameters are $a = 1.66175$, $b = -8.5166$, $c = -0.20228$, and $d = -33.9069$. Another set of parameters referred to as VSS2 herein are taken from⁶² where the values are $a = 1.3892$, $b = 13.862$, $c = -0.1086$ and $d = -41.458$. The hindrance factor h is set to 0 for even-even nuclei in both cases.

2.2.2. Parkhomenko-Sobiczewski (PS) formula

Parkhomenko and Sobiczewski^{62,63} dropped the parameter b from equation 6 and refitted the resulting half-life equation:

$$\log_{10} T_{1/2}^{PS} = aZQ_\alpha^{-\frac{1}{2}} + bZ + c, \quad (7)$$

using the same 61 nuclei with $Z = 84 - 110$ and $N = 128 - 160$. The retained values for the adjustable parameters are $a = 1.5372$, $b = -0.1607$ and $c = -36.573$. The root-mean-square (r.m.s) was reported to differ only very slightly as compared to the four parameters set of VSS2.

2.2.3. Royer (R) and modified Royer (mR) formulas

The Royer's formula⁶⁴ developed based on the liquid drop model is given by the expression:

$$\log_{10} T_{1/2}^R = aZQ^{-\frac{1}{2}} + bA^{\frac{1}{6}}Z^{\frac{1}{2}} + c. \quad (8)$$

We selected the values of adjustable parameters corresponding to the fit to 131 even-even alpha emitters⁶⁴ with $a = 1.5864$, $b = -1.1629$, and $c = -25.31$.

We have also considered a modified Royer formula developed by⁶⁵ where the angular momentum of the α -particle is taken into account. The modified formula takes the form of

$$\log_{10} T_{1/2}^{mR} = aZQ^{-\frac{1}{2}} + bA^{\frac{1}{6}}Z^{\frac{1}{2}} + c + d \frac{(ANZ[l(l+1)]^{\frac{1}{4}})}{Q} + eA[1 - (-1)^l]. \quad (9)$$

For the case of ground-state-to-ground-state transition between the parent and daughter nuclei, the angular momentum l carried by the alpha particle is zero. Therefore, the last two terms on the right-hand side of equation (9) vanishes in our case. This gives rise to the same expression given in equation (8) with only a slight difference in the values of the adjustable parameters. We employed the values of $a = 1.58439$, $b = 1.15847$, $c = -25.31$ fitted to 137 even-even nuclei in the work of⁶⁶.

2.2.4. Brown and modified Brown formulas

The Brown's formula⁶⁷ for alpha decay half-life is given by:

$$\log_{10} T_{1/2}^{BF} = 9.54(Z-2)^{0.6}Q^{-\frac{1}{2}} - 51.37, \quad (10)$$

whereby parameters were fitted to alpha emitters in the $Z = 76 - 108$ and $N = 90 - 156$ region.

We have also considered two modified Brown formula proposed by⁶⁸ fitted to 96 superheavy nuclei. The first formula referred to as MB1 given by the expression:

$$\log T_{1/2}^{MB1} = a(Z-2)^b Q^{-\frac{1}{2}} + c + h, \quad (11)$$

and was fitted by considering a , b and c to be the same for all sample nuclei while the hindrance factor h to be dependent on whether the neutron and proton numbers are even or odd. The parameters for MB1 are $a = 13.0705$, $b = 0.5182$ and $c = -47.8867$, while h for even-even nuclei is set to 0.

The second modified Brown formula⁶⁸ is given as:

$$\log T_{1/2}^{MB2} = a(Z-2)^b Q^{-\frac{1}{2}} + c, \quad (12)$$

and was fitted without the hindrance factor but separated into four different sets corresponding to even-even, odd-even, even-odd and odd-odd nuclei. For the set of even-even nuclei, the parameters are $a = 10.8238$, $b = 0.5966$, and $c = -56.9785$.

2.3. Two-nucleon separation energy and separation energy differential

The two-nucleon separation energy calculated using the equation (for the case of neutron):

$$S_{2n}(N, Z) = E_B(N-2, Z) - E_B(N, Z), \quad (13)$$

where $E(N, Z)$ is the binding energy of the nucleus with Z protons and N neutrons is a frequent observable used to locate magic numbers.

The variation of the separation energy with consecutive nucleon number is another way in which one can determine magic numbers for e.g. as in the studies of^{5,15,69}. We refer to this quantity as the two-nucleon separation energy differential δS_{2q} .

As an example in the case of neutrons, the δS_{2n} is calculated using the equation:

$$\delta S_{2n} = S_{2n}(N, Z) - S_{2n}(N + 2, Z). \quad (14)$$

The δS_{2q} herein refers to the same quantity known as two-nucleon gap in⁵ given in terms of the three-point formula in the case of neutrons by:

$$\delta S_{2n}(N, Z) = 2E_B(N, Z) - E_B(N - 2, Z) - E_B(N + 2, Z). \quad (15)$$

3. Results and Discussions

3.1. Location of the ground-state deformation β_{20}

We first performed multiple constrained calculations by fixing electric quadrupole moment (Q_{20}) while restricting only to axial and parity symmetric nuclear shapes. The location of ground-state (g.s.) deformation is then obtained by releasing the constraint on Q_{20} from the solution closest to where the minimum is expected.

We plotted a contour map of the ground-state β_{20} as a function of neutron number, N in the range of $170 \leq N \leq 190$ and proton number, Z in the range of $112 \leq Z \leq 130$ in Figure 1. The dimensionless deformation parameter β_{20} is derived from the quadrupole moment Q_{20} given as⁷⁰:

$$\beta_{20} = \frac{4\pi}{5} \frac{Q_{20}}{A\langle r^2 \rangle} \quad (16)$$

where $\langle r^2 \rangle$ is the root-mean-square radius (*rms*), $\frac{4\pi}{5}$ the scaling factor and A the mass number.

All Skyrme parametrizations showed almost the same pattern in the evolution of the ground-state shape with a major distinction in the lower left region of the plot. While all of the Skyrme parametrizations predict that nuclei located in the lower left region is prolate, the region with prolate deformation is significantly larger in the case of SLy5 and SLy4 (up to around $Z = 118$ and $N = 176$) as compared to SkM* (around $Z = 114$ and $N = 170$).

Apart from that, another minor difference is in terms of the on-set of sphericity around $N = 184$. For the SkM* and SLy5 parametrization, nuclei in the region around $114 \leq Z \leq 120$ are expected to be spherical starting at $N = 182$. However, sphericity is only achieved in the case of the SLy4 parametrization at $N = 184$ although the deformation at $N = 182$ is rather small. On the far right region at $Z = 130$ and $N = 190$ all of the considered Skyrme parametrizations predicted a rather rigid oblate deformation.

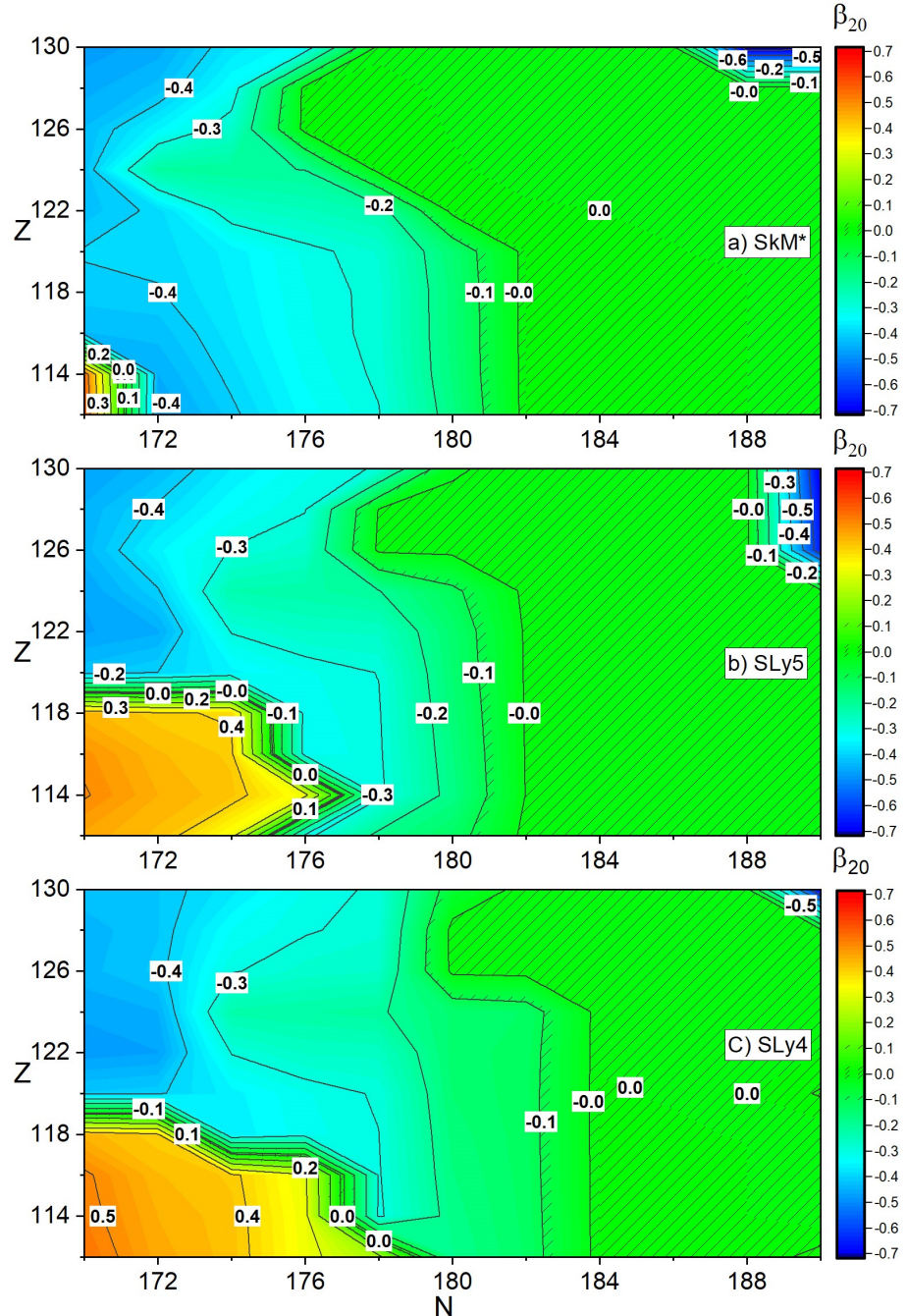


Fig. 1. Contour map showing the location of the ground-state electric quadrupole moment (in dimensionless β_{20}) as a function of neutron N and proton Z numbers. Negative (positive) values indicate an oblate (prolate) shapes while $\beta_{20} = 0$ indicate a spherical shape.

3.2. Binding energy per nucleon at the ground-state deformation

We tabulated the ground-state binding energy per nucleon (BE/A in absolute value) obtained in our calculations with those of Ref.⁷¹ using the same Skyrme parametrizations but within the Hartree-Fock-Bogoliubov (HFB) approach in Table 4. In their calculations, the density-dependent delta pairing force was employed.

We find that our results agree well with the HFB results where the differences in BE/A are, on average, about 14 keV for SkM* and SLy4, and about 25 keV for SLy5. Figure 2 shows the evolution of BE/A as a function of mass number A . In most cases, our calculated data shows the same trend as those obtained in the work of Ref.⁷¹ The only difference in the trend from one nucleus to another between our results and theirs appear between the ^{290}Lv and ^{292}Lv nuclei. The HFB calculations showed a sudden drop in BE/A with the SLy4. This is not visible in our BE/A results which varies smoothly with A . Some tests have been performed, but the same pattern persists.

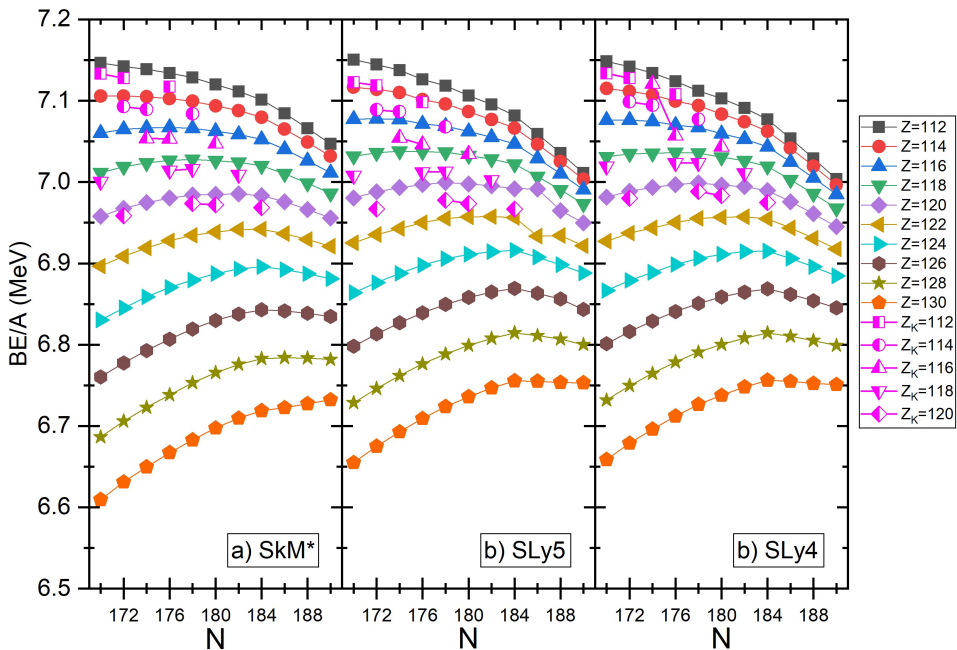


Fig. 2. Shows plots of binding energy per nucleon (BE/A) for all Skyrme parametrization considered herein for $112 \leq Z \leq 130$. The obtained values are compared to the work of Ref.⁷¹ represented in half-filled magenta color.

3.3. Root-mean-square and charge radii

We tabulated the root-mean-square radii ($r_{rms} = \sqrt{\langle \hat{r}^2 \rangle}$) and proton radius ($r_p = \langle \hat{r}_p^2 \rangle$) in Table 5 and Table 6 and plotted it in Fig. 3 for easy comparison. We find that the r_{rms} increases smoothly with A as expected. However, there appears a jump in r_{rms} for nuclei at the end of the isotopic chain of $Z = 130$ (SkM*), $Z = 126, 128, 130$ (SLy5) and $Z = 128, 130$ (SLy4). The change in r_{rms} corresponds to the change in the ground-state deformation as seen in Fig. 1 at the corresponding neutron and proton numbers. Similarly, the sudden jump in the case of r_p occurs at the point where there is a change in the ground-state deformation.

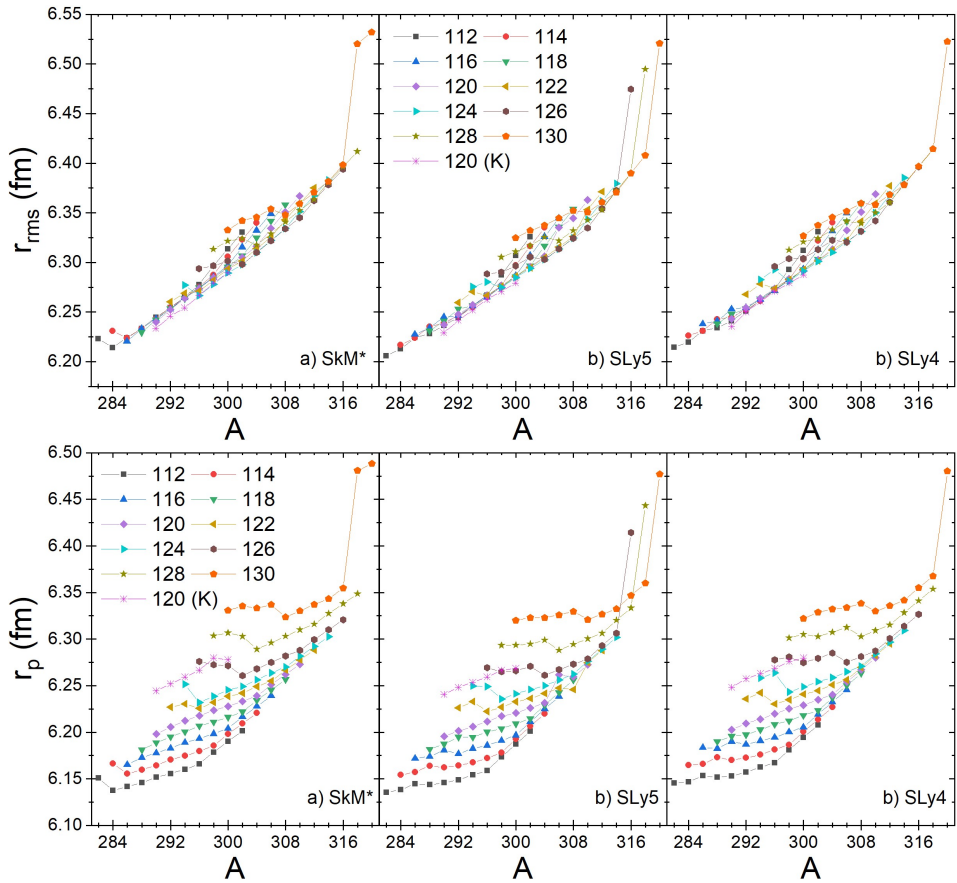


Fig. 3. Top plots shows root-mean-square radii (r_{rms}) and bottom plots proton radius (r_p) for sample nuclei and Skyrme forces considered herein. The obtained values for $Z = 120$ are compared to the work of Ref.⁷¹ represented in star-like marker in magenta color.

It should be noted that the increase in r_{rms} and r_p is strongly affected by the choice of pairing strengths. Fig. 4 shows a comparison of r_{rms} (middle panel) and

r_p (bottom panel) for $Z = 130$ isotopes obtained with two different sets of pairing strengths. When $(G_n, G_p) = (16.72, 14.25)$ MeV are chosen, we find a jump in both r_{rms} and r_p at $N = 190$ (corresponding to $A = 320$ in Fig. 3). However, the r_{rms} and r_p varies smoothly with N when lower values of $(G_n, G_p) = (14.79, 13.72)$ MeV are employed. This reiterates the importance of proper selection of pairing strengths. Further study along the work of one co-author⁷² could be explored in future work.

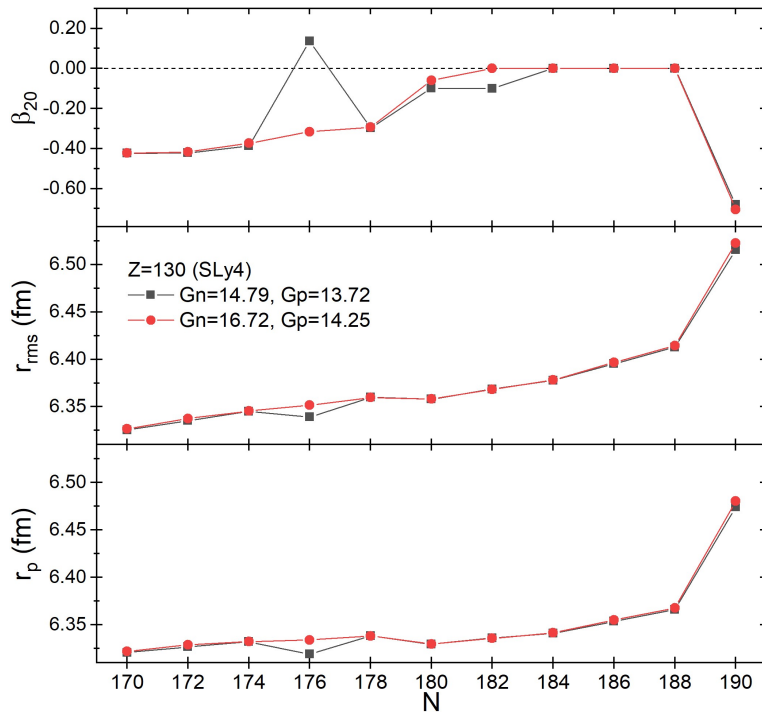


Fig. 4. The figure shows plots for (a) root-mean-square radii (r_{rms}) and (b) charge radii r_p (fm) for SLy4 parametrization for $Z = 130$. The obtained values are compared to the work of Ref.⁷¹ represented in half-filled magenta color.

In the earlier work,⁷¹ similar calculations for $Z = 120$ isotopes have been performed where the charge radius r_{ch} had been calculated using $r_{ch} = \sqrt{r_p^2 + 0.64}$. These values obtained within the Hartree-Fock-Bogoliubov (HFB) framework are plotted in Fig. 3 for comparison. Apart from the constant $0.8^2 = 0.64$ to account for the finite size of the proton, we find that the trend for the $Z = 120$ isotopes from the HFB calculations are similar to our results.

3.4. Two-nucleon separation energy differential δS_{2q}

Figure 5 shows the two-neutron separation energy differential δS_{2n} and two-proton separation energy differential δS_{2p} . Simultaneous evaluation of both quantities is necessary to pinpoint the emergence of shell closures, as suggested by⁵. It is obvious from Figure 5 that all three Skyrme forces predict $Z = 126$ and $N = 184$ to be the next spherical magic numbers after $Z = 82$ and $N = 126$, this has indeed been proposed by many for e.g.^{5, 73, 74}.

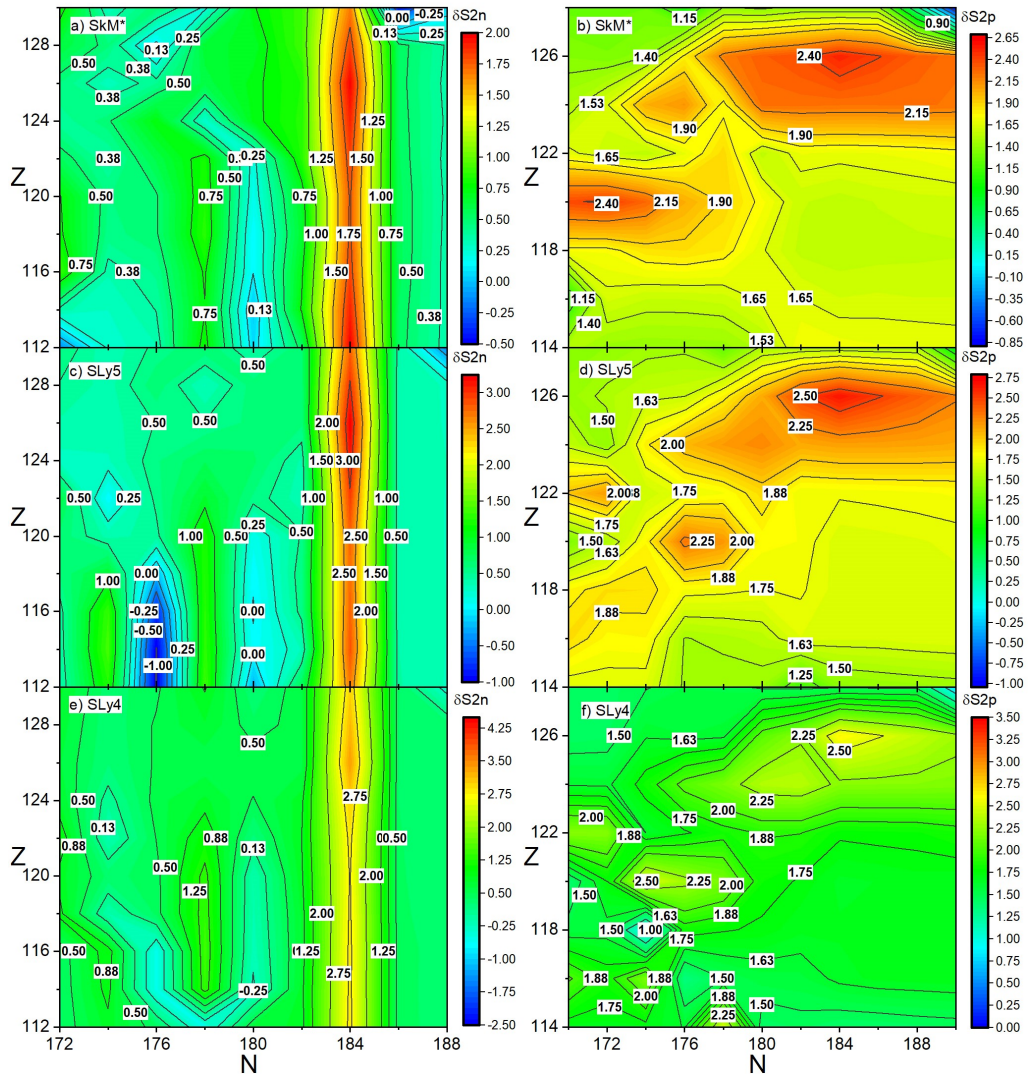


Fig. 5. Shows contour mapping of δS_{2n} left panel and δS_{2p} panel. Skyrme parametrizations calculated shown at different rows (top) for SkM*, (middle) SLy5 and (bottom) SLy4.

Beyond this set of spherical magic numbers, there also appears regions with relatively high δS_{2q} . Comparing the contour of δS_{2n} (left panels) of Figure 5, there appears a ridge at $N = 178$ from $Z = 112$ to 122 for all Skyrme forces. In addition to $N = 178$, the SLy5 parametrization also predicts a region with high δS_{2n} at $N = 174$ starting from $Z = 112$ to 118. The SLy4, however, shows only a small region of high δS_{2n} at $N = 174$ for $Z = 114$ and 116. The region of high δS_{2n} then shifted towards $N = 172$ and moving upwards from $Z = 118$ towards $Z = 130$.

For protons, the δS_{2p} of Figure 5 (right panels) shows a region with high δS_{2p} comparable to the spherical magic number of $Z = 126$ at $Z = 120$ for $N = 172$ (SkM*), $N = 176$ (SLy5), and $N = 174$ (SLy4). For the SLy4, an even intense peak is seen at around $Z = 114$, $N = 174$ suggesting a potentially relatively stable isotope due to proton magicity. This is however not seen with the other two Skyrme forces.

Evaluating Figure 5 with respect to the Q_{20} plot in Figure 1, we identify $N = 178$ as a *deformed magic number* from $Z = 114$ to 120 with an oblate ground-state shape. The emergence of $N = 174$ as deformed magic number predicted with the SLy5 and SLy4 appears at the prolate side of the deformation. Similarly, the intense peak at $Z = 114$, $N = 174$ predicted only with the SLy4 has the same deformation type. On the other hand, the region with high δS_{2n} at $N = 172$ from $Z = 118$ to $Z = 130$ predicted with the SLy4 has a prolate shape at $Z = 118$ which then shifted to an oblate shape starting at $Z = 120$.

For protons, the SkM* parametrization predicted a deformed magic number at $Z = 120$ around $N = 172$ with a rather strong oblate ground-state shape, and $Z = 124$ around $N = 176$ with a slightly oblate ground-state shape. The SLy5 parametrization predicted the location of deformed magic number at the same proton number but with different neutron number namely at $Z = 120$ around $N = 176$, and, $Z = 124$ around $N = 180$ with similar ground-state deformations as obtained with the SkM* parametrization. The SLy4 predicts deformed proton magic number at $Z = 114$ around $N = 174$ with a prolate shape, while $Z = 120$ with $N = 174$ and at $Z = 122$ with $N = 172$ with an oblate shape.

3.5. Single-particle levels

Figure 6 shows comparison of the single-neutron and single-proton levels at the oblate, spherical and prolate shapes for $^{288}\text{Fl}_{174}$ nucleus obtained with the SkM* and SLy5 parametrizations. Here we show that the appearance of ridges in the δS_{2n} and δS_{2p} plots is attributed to a substantial energy gap in the single-particle levels at the relevant nucleon numbers.

For neutrons, the SkM* parametrization shows that energy gaps for $N = 174$ at the prolate deformation while the SLy5 parametrization shows a substantial gap at the same neutron number on the oblate side with an even larger gap at the prolate deformation. Conversely, the region with large δS_{2n} around $N = 178$ is attributed to the large energy gap in the single-particle levels.

For protons, it is clear that the high δS_{2p} at $Z = 120$ (with oblate ground-state) obtained with both parametrizations is due to the large energy gap in the single-particle levels at $Z = 120$. On the other hand, a substantial energy gap at $Z = 124$ on the oblate side with the SLy5 parametrization is not seen in the plot for $^{288}\text{Fl}_{174}$ nucleus. Instead, the energy gap at $Z = 124$ appears at around $N = 180$ as seen in bottom single panel of Figure 6.

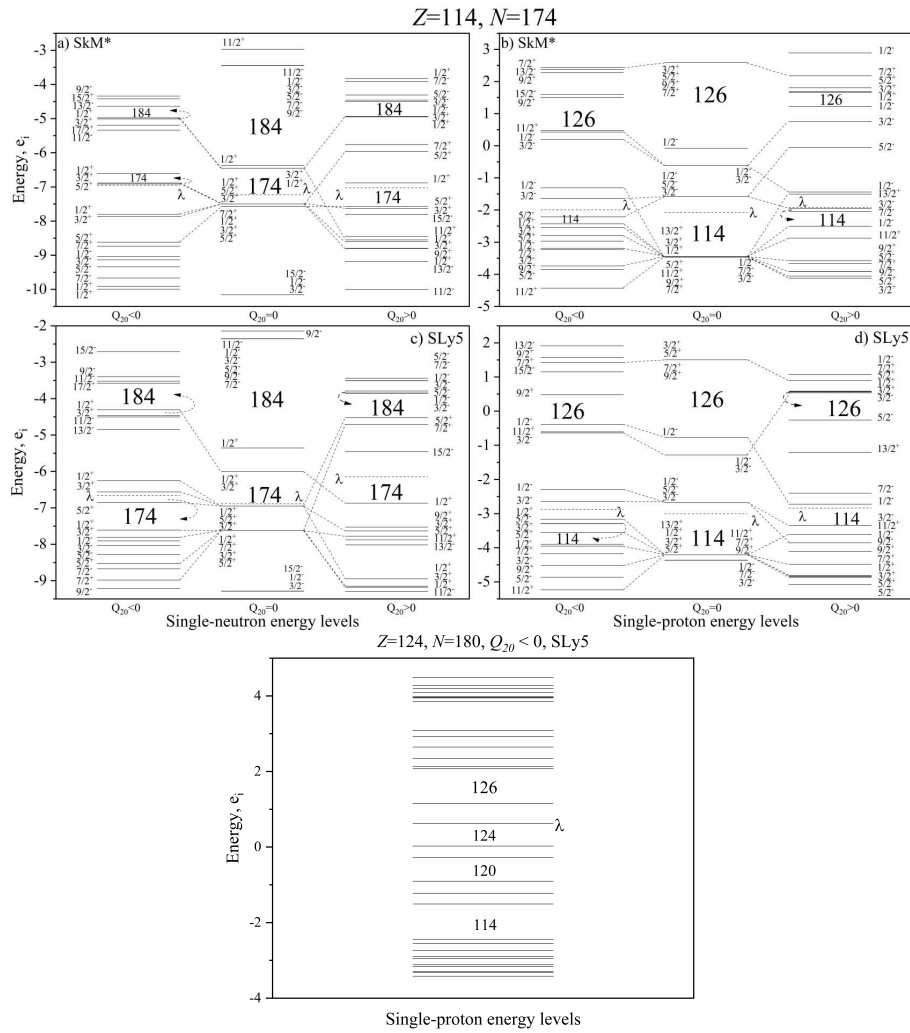


Fig. 6. Single-particle levels at the oblate ($Q_{20} < 0$), spherical ($Q_{20} = 0$) and prolate ($Q_{20} > 0$) minimum obtained with the SkM* and SLy5 parametrizations for the $Z = 114$, $N = 174$ nucleus. The single bottom panel shows proton single-particle levels obtained with the SLy5 parametrization for the $Z = 124$ and $N = 180$ nucleus showing an energy gap at $Z = 124$ which does not appear in Figure 6 for the case of $N = 174$.

Apart from the above, we also note that both Skyrme parametrizations show large energy gap in the single-particle energy levels at sphericity for $Z = 126$ and $N = 184$. This reinforce the candidacy of $^{310}126_{184}$ as a doubly magic nucleus after $^{208}_{82}\text{Pb}_{126}$.

3.6. Energy released in alpha-decay Q_α

The Q_α values calculated using equation (5) with the ground-state energies as inputs, are tabulated in Table 7 and plotted against neutron number in Figure 7.

In Figure 7, a peak can be seen at $N = 186$ for all the isotopes $114 \leq Z \leq 130$ in all Skyrme parametrization plotted in panel (a), (b), and (c). This lends further support to $N = 184$ (corresponding to the daughter nucleus after the alpha decay) as a strong candidate for spherical magic number, as was claimed by many previous studies (see Table 1).

Furthermore, it is interesting to point-out that a peak appears at $N = 180$ at lighter SH nuclei around $114 \leq Z \leq 122$ for SkM* and SLy5, and $116 \leq Z \leq 124$ for SLy4, except $Z = 114$. This suggest that $N = 178$ is a candidate of deformed magic number, as was recently claimed by^{32,47}. Figure 2 of Ref.³² showed magicity at $N = 178$ and $N = 184$ for isotopic series $Z = 118, 119$, and 120.

On the other hand, the Q_α of even-even isotopes presented in Figure 4(b) in Ref.⁷⁶ showed possible magicity at $N = 178$ for $116 \leq Z \leq 124$, and $N = 184$ for $114 \leq Z \leq 126$. It was also suggested that $^{296}118$ and $^{298}120$ with both having $N = 178$ are much more stable in configuration with calculated oblate (deformed) shape.

Comparing the calculated values to the limited experimental data available in the nuclear region, it appears that the SkM* parametrization correctly reproduced the experimental downward trend for $172 \leq N \leq 176$ in the $Z = 114$ and $Z = 116$ isotope chains.

Nonetheless, the SLy5 and SLy4 predicted a peak in the alpha energy at $N = 176$ for selected isotopes, but this was not observed in the experiment. The $N = 176$ Q_α peak obtained with the SLy5 and SLy4 parametrization is due to an energy gap in the single-particle spectra at $N = 174$ resulting in the emergence of a peak in the two-neutron separation energy differential. As for the SLy4 parametrization shows peaks at $N = 174$ for $Z = 124$ and 126 indicating that $N = 172$ to be magic.

The fact that the all three Skyrme parametrizations gave conflicting results with respect to the possibility of $N = 172$ and 174 sub-magic numbers is interesting. We note that^{7,11,52} has also predicted a shell closure at these neutron numbers. However, this point could only be verified through further experimental exploration.

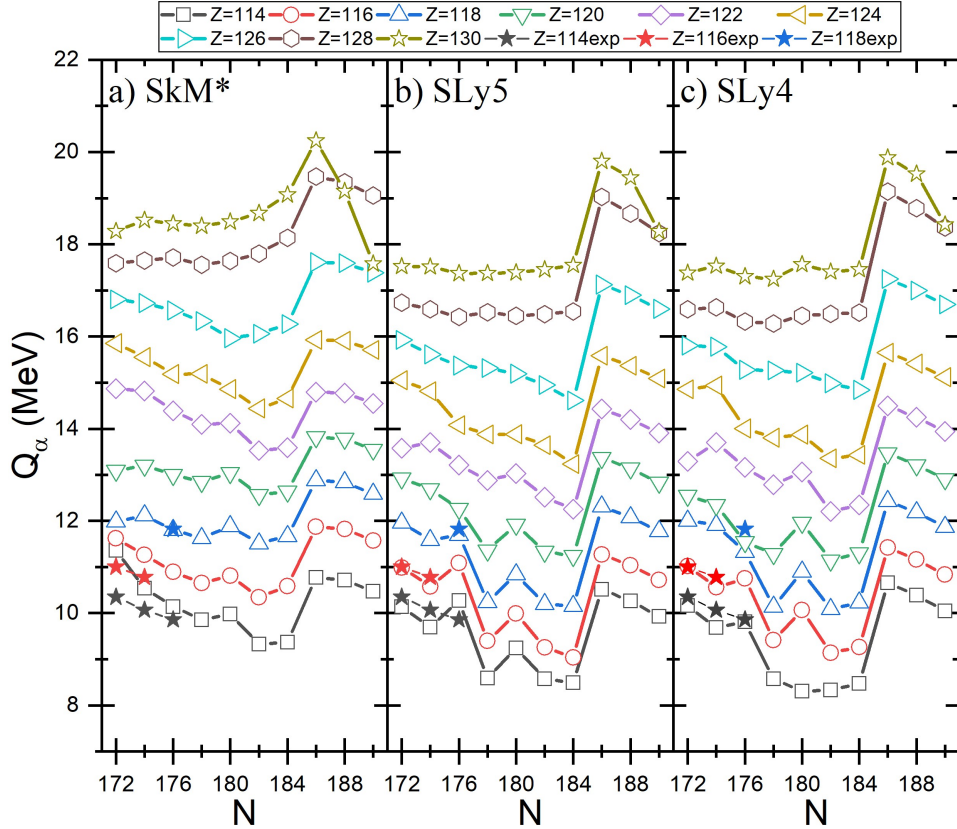


Fig. 7. Alpha-decay energies, Q_α -values (in MeV) for isotopic series $114 \leq Z \leq 126$ and $172 \leq N \leq 190$ for the SkM*, SLy5, and SLy4 Skyrme parametrizations as a function of N . Available experimental values taken from⁴ and⁷⁵ are plotted in star shaped according to their designated colour.

3.7. Alpha-decay half-life $T_{1/2}$

Using the Q_α values obtained with averaged pairing strengths (given in Table 2), we calculated the logarithmic α -decay half-lives ($\log_{10} T_{1/2}$) using various semi-empirical formulae as listed in Sec. 2.2. The calculated values using SkM*, SLy5 and SLy4 parametrizations are listed in Table 8, Table 9 and Table 10 , respectively.

We found that the nucleus with the longest $\log_{10} T_{1/2}$ within our samples to be the $Z = 114$ isotopes at $N = 180$ (SLy4), $N = 184$ (SLy5), and $N = 182$ (SkM*).

This finding reiterate the conclusion based on the single particle spectra (shell gaps) of Refs.^{5,7} and alpha decay half-life of Refs.^{10,47} which shows high stability for the $Z = 114, N = 184$ albeit a slight deviation in our case with the SLy4.

Figure 8 shows the evolution of our calculated $T_{1/2}$ based on the VS1 formula and superimposed with g.s. β_{20} heatmap. In panel (a) of the figure obtained with the SkM* parametrization, peaks in the $\log_{10} T_{1/2}$ are seen various neutron and proton

numbers namely at $N = 178$ with $Z = 114 - 122$, $N = 182$ with $Z = 114 - 124$ and $N = 184$ with $Z = 114 - 122$. It is interesting to note here that the $N = 184$ loses its magic character at around $Z = 128$ and beyond. This can be clearly seen in Figure 9 which was plotted using the average $\log_{10} T_{1/2}$ of the eight semi-empirical formulas. Contrast this to the results obtained with the SLy5 and SLy4 parametrization in panel (b) and (c) where $N = 182$ is not magic while $N = 184$ remains as a magic number for all Z numbers considered herein. In addition to $N = 178$, a relatively high peak is seen at $N = 174$ with the SLy5 and SLy4 parametrizations.

Comparing the location of magic numbers with the g.s. deformation, we find that the $N = 178$ between $Z = 114 - 122$ forms a deformed (oblate) magic nuclei for all Skyrme parametrizations. For $N = 182$, we found that the $Z = 114 - 124$ forms a (spherical) shell closure with the SkM* parametrizations, whereas $N = 184$ is spherical for all Skyrme parametrizations. In panel (b) and (c) obtained with the SLy5 and SLy4 parametrization, we found that $N = 174$ could be a candidate for a deformed (prolate) magic number.

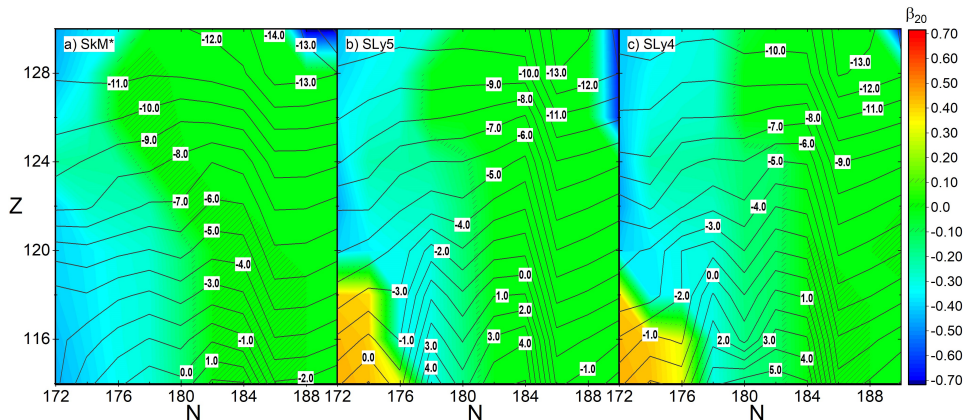


Fig. 8. Shows overlapped between the ground-state β_{20} given in color and the alpha-decay half-life $\log_{10} T_{1/2}$ from VS1 given in terms of contour lines. Nuclei along the isotone $N = 184$ exhibit spherical ground-state and therefore is a spherical magic number.

In what follows, we keep our analyses to quantities which are taken as average of half lives obtained with the 8 semi-empirical formulas discussed in Sec 2.2. Further discussion on the differences between results of the different formulas are provided in the Appendix A.

These averaged $\log_{10} T_{1/2}$ values are plotted as a function of N in Figure 9. The largest negative and positive differences with respect to the averaged values are plotted as error bars to indicate the uncertainties in semi-empirical formulae.

The $\log_{10} T_{1/2}$ systematic plots in Figure 9 compliments the observation from Figure 8 by showing magic candidate peaks at $N = 178$ and 182 or 184, where there appears a sharp decrease in the alpha decay $T_{1/2}$ when going from $N = 184$ to $N =$

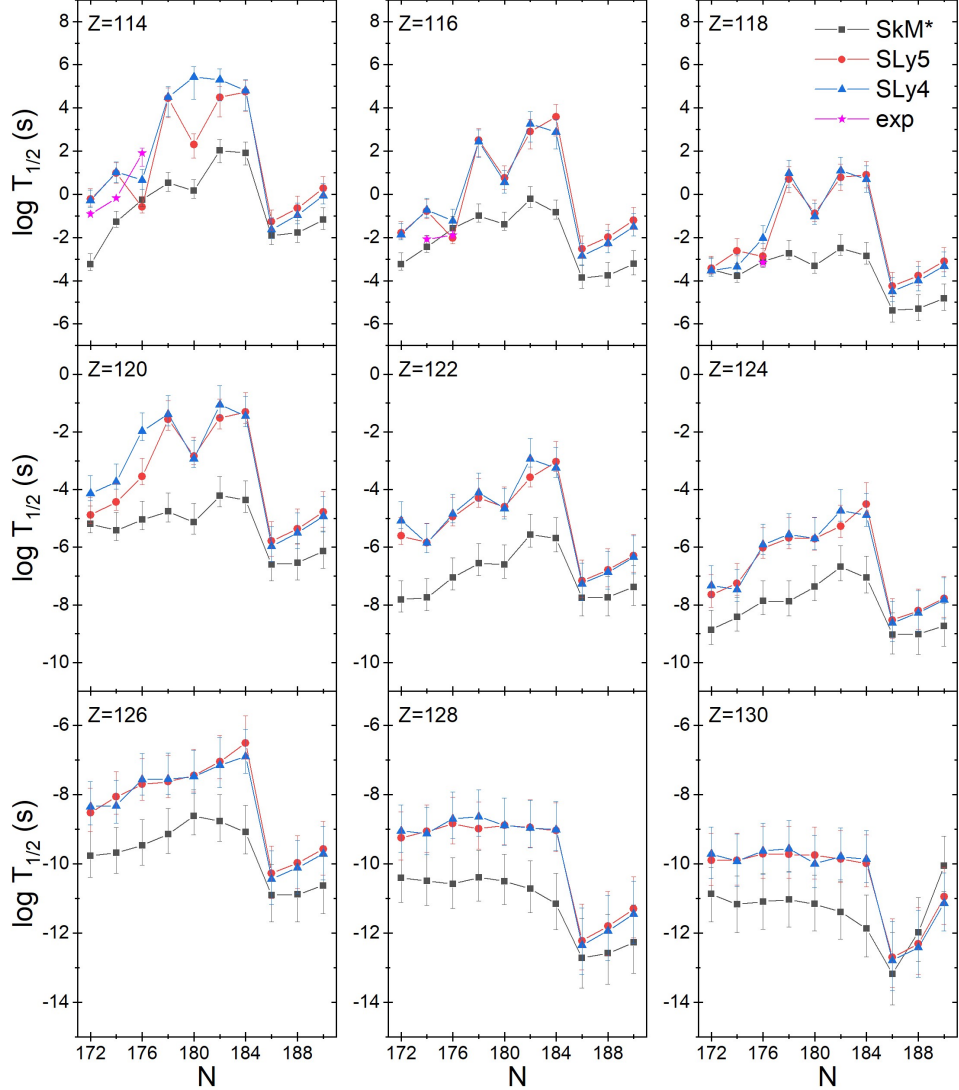


Fig. 9. Shows the $\log_{10} T_{1/2}$ of all Skyrme parametrization are plotted from averaged of 8 different formulae against (N) and the error bar are the maximum and minimum $T_{1/2}$ range for isotopic series $114 \leq Z \leq 130$ ($172 \leq N \leq 190$). The experimental $\log T_{1/2}^{\alpha}$ are plotted using magenta star symbol⁷⁵.

186 for all Skyrme parametrizations. The experimental $\log_{10} T_{1/2}$ for $Z = 114 - 118$ are shown in the same figure. Interestingly, SkM* parametrization $\log_{10} T_{1/2}$ trends are consistent with $\log_{10} T_{1/2}^{\exp.}$, which suggest that $N = 174$ ($Z = 114 - 118$) is not a magic number candidate contrary to the findings obtained with the SLy5 and SLy4 parametrizations and also in the recent study of by Malov et al.⁵²

It is also interesting to note that our calculations showed a rather different pattern in alpha-decay half-life for $N \geq 188$ as compared to Figure 4 of⁷⁷. In⁷⁷, the authors predicted that the alpha-decay half-life of $Z = 126$ with $N = 188$ nucleus to be higher than the half-life of the doubly magic nucleus $^{310}126_{184}$ by about 2 orders of magnitude. In our calculations, we found that alpha-decay half-life for $186 \leq N \leq 190$ is always lower than its neighbour $N = 184$ for any Z isotopes, except for $Z = 130$ obtained using SkM* parametrization.

We now move on to discuss the magic number candidates for protons. To this end, we plotted the difference in the half-life of $\log_{10} T_{1/2}$, ($\delta \{\log_{10} T_{1/2}(Z)\}$), as a function of proton number Z as shown in Figure 10 with fixed $N = 172 - 178$, and 184 using the equation:

$$\delta \{\log_{10} T_{1/2}(Z)\} = \log_{10} T_{1/2}(Z) - \log_{10} T_{1/2}(Z + 2). \quad (17)$$

In panel (a) of Figure 10 obtained with the SkM* parameterization, a sharp peak appears in $\delta \{\log_{10} T_{1/2}(Z)\}$ at $Z = 120$ for $N = 172$ and 174, and another small peak at $Z = 124$ for $N = 174$ and 176. This is associated to the region with high and moderate δS_{2p} in panel (c) of Figure 5 at the corresponding Z and N numbers. The peak appears instead at $Z = 126$ and with possibly another higher peak around $Z = 114$ corresponding to a small region of high $\log T_{1/2}$ in Figure 8.

Next, in the similar plot for the SLy5 and SLy4 parametrization plotted in panel (b) and (c) the peaks in ($\delta \{\log_{10} T_{1/2}(Z)\}$) appears at $Z = 120$ similar to what was obtained with the SkM* parameterization but at different neutron number namely $N = 176$ and 178 for SLy5, and $174 \leq Z \leq 178$ for SLy4. For $N = 184$, no peak is observed at $Z = 120$. Instead, a slight peak appears at $Z = 116$ and a more pronounced peak appears at $Z = 126$.

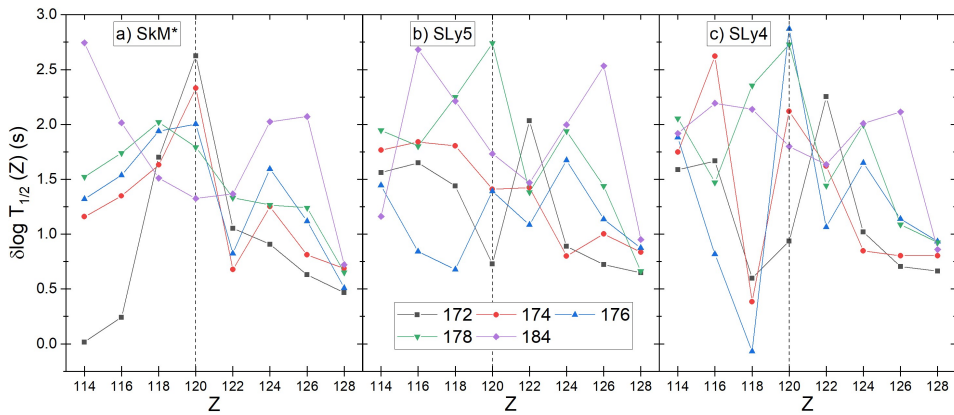


Fig. 10. Shows difference in alpha-decay half-life $\log_{10} T_{1/2}$ as a function of N for proton number $Z = 120$ and function of Z for neutron number $N = 178$ obtained with all Skyrme parametrization.

4. Conclusion

In this article, we presented our calculations based on the Skyrme Hartree-Fock-plus-BCS framework for superheavy nuclei in the region of $112 \leq Z \leq 130$ and $172 \leq N \leq 190$. The aim is to identify the candidates for neutron and proton magic numbers by simultaneously evaluating the single-particle properties via two-nucleon separation energy differential and single-particle energy levels, and the bulk properties via Q_α energy and alpha-decay half-life $\log_{10} T_{1/2}$.

We found that $N = 178$ to be a candidate for neutron deformed magic number around $114 \leq Z \leq 118$, but not for $N = 174$. This finding is supported by the emergence of peaks in the $\log_{10} T_{1/2}$ as a function of N , and the two-neutron separation energy differential δS_{2n} . Emergence of this deformed magic number is supported by a significant energy gap in the single-particle energy levels with an oblate ground-state shape. While results obtained with the SLy5 and SLy4 show a potential deformed magic number at $N = 174$, the actual magic character at $N = 174$ may be unlikely based on the trend in the experimental alpha decay energies and half-life.

For protons, we found that $Z = 120$ and 124 to be a candidate for deformed magic number at around $N = 172 - 176$ (with the SkM*), $N = 176 - 178$ (with the SLy5), and $N = 174 - 178$ (with the SLy4). This was identified from the analyses of two-proton separation energy differential δS_{2p} and reconfirmed from the analyses of the variation in the alpha-decay half-life $\delta \log T_{1/2}$ as a function of Z number.

In addition to deformed magic numbers, we have also found simultaneous peaks in the δS_{2n} and δS_{2p} at $N = 184$ and $Z = 126$, respectively. Coupled with the fact that the ground-state deformation was found at sphericity, we arrived at the same conclusion as was found before, that $^{310}126_{184}$ is a doubly magic nucleus.

The information presented herein is of interest in the effort to synthesize new superheavy elements. Figure-11 illustrates the locations for nuclei that could be of interest within the superheavy region. In particular are nuclei around (i) $Z = 114 - 116$ with $N = 184$, (ii) $Z = 118$ with $N = 178$ (iii) $Z = 120$ around $N = 172 - 178$, (iv) $Z = 122 - 124$ with $N = 172 - 178$.

Acknowledgements

The authors would like to acknowledge the Ministry of Education Malaysia for the financial support through the Fundamental Research Grant Scheme (FRGS/1/2018/ST/G02/UTM/02/6), and UTM (R.J130000.7854.5F028).

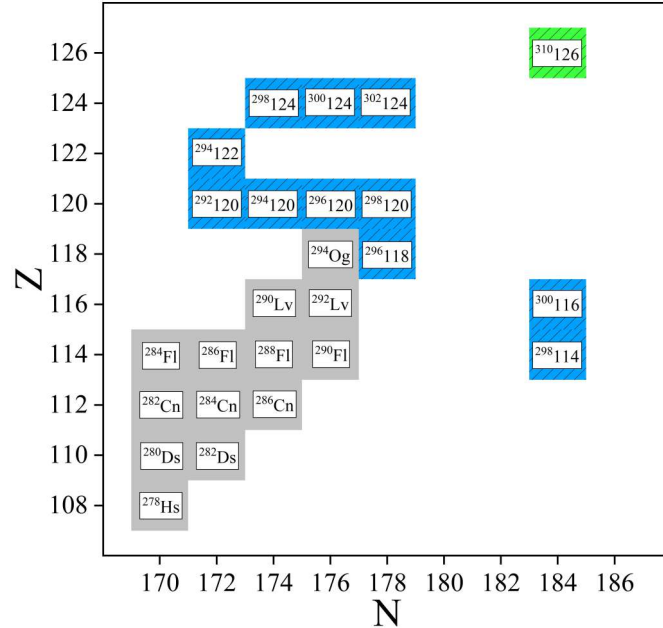


Fig. 11. Shows even-even nuclei in the superheavy region of nuclear chart. The boxes in grey represents known synthesized nuclei while boxes in blue are suggested candidates nuclei for exploring the superheavy region towards the doubly magic $^{310}\text{126}$ in green.

Table 4: Binding energy per nucleon BE/A obtained in current work with the SkM*, SLy5 and SLy4 parametrizations and compared with the results obtained from Ref.⁷¹ using the Skyrme HFB framework.

Z	N	A	BE/A					
			SkM*	SLy5	SLy4	SkM*	SLy5	SLy4
			(HFB)	(HFB)	(HFB)			
112	170	282	7.147	7.151	7.148	7.133	7.123	7.134
112	172	284	7.142	7.145	7.142	7.128	7.119	7.128
112	174	286	7.139	7.138	7.134	—	—	—
112	176	288	7.134	7.126	7.124	7.117	7.098	7.108
112	178	290	7.128	7.119	7.112	—	—	—
112	180	292	7.120	7.106	7.103	—	—	—
112	182	294	7.111	7.095	7.091	—	—	—
112	184	296	7.101	7.082	7.077	—	—	—
112	186	298	7.085	7.059	7.054	—	—	—

Table 4 – *Continued on next page*

Table 4 – *Continued from previous page*

Z	N	A	BE/A					
			SkM*	SLy5	SLy4	SkM* (HFB)	SLy5 (HFB)	SLy4 (HFB)
112	188	300	7.066	7.036	7.029	–	–	–
112	190	302	7.047	7.011	7.004	–	–	–
114	170	284	7.106	7.117	7.115	–	–	–
114	172	286	7.106	7.114	7.112	7.093	7.089	7.099
114	174	288	7.105	7.110	7.107	7.089	7.086	7.094
114	176	290	7.103	7.101	7.099	–	–	–
114	178	292	7.099	7.096	7.094	7.084	7.068	7.077
114	180	294	7.094	7.086	7.083	–	–	–
114	182	296	7.088	7.077	7.074	–	–	–
114	184	298	7.080	7.066	7.062	–	–	–
114	186	300	7.065	7.046	7.041	–	–	–
114	188	302	7.049	7.025	7.019	–	–	–
114	190	304	7.032	7.003	6.997	–	–	–
116	170	286	7.060	7.077	7.076	–	–	–
116	172	288	7.065	7.078	7.076	–	–	–
116	174	290	7.067	7.077	7.075	–	–	–
116	176	292	7.067	7.072	7.070	7.054	7.054	7.121
116	178	294	7.066	7.069	7.067	7.053	7.046	7.057
116	180	296	7.063	7.062	7.060	–	–	–
116	182	298	7.059	7.055	7.053	7.048	7.034	7.043
116	184	300	7.052	7.047	7.043	–	–	–
116	186	302	7.040	7.029	7.025	–	–	–
116	188	304	7.026	7.010	7.005	–	–	–
116	190	306	7.011	6.991	6.985	–	–	–
118	170	288	7.012	7.032	7.031	7.001	7.008	7.019
118	172	290	7.019	7.036	7.035	–	–	–
118	174	292	7.024	7.038	7.035	–	–	–
118	176	294	7.027	7.037	7.036	7.014	7.012	7.024
118	178	296	7.028	7.037	7.036	7.016	7.013	7.023
118	180	298	7.026	7.033	7.031	–	–	–
118	182	300	7.024	7.028	7.026	7.009	7.003	7.011
118	184	302	7.020	7.022	7.019	–	–	–
118	186	304	7.010	7.007	7.003	–	–	–
118	188	306	6.999	6.990	6.986	–	–	–
118	190	308	6.986	6.973	6.968	–	–	–
120	170	290	6.958	6.980	6.981	–	–	–

Table 4 – *Continued on next page*

Table 4 – *Continued from previous page*

Z	N	A	BE/A					
			SkM*	SLy5	SLy4	SkM* (HFB)	SLy5 (HFB)	SLy4 (HFB)
120	172	292	6.968	6.988	6.989	6.959	6.967	6.980
120	174	294	6.975	6.993	6.993	–	–	–
120	176	296	6.980	6.997	6.997	–	–	–
120	178	298	6.984	7.000	6.999	6.974	6.978	6.989
120	180	300	6.985	6.998	6.996	6.972	6.973	6.983
120	182	302	6.985	6.996	6.994	–	–	–
120	184	304	6.983	6.992	6.990	6.969	6.967	6.975
120	186	306	6.976	6.991	6.976	–	–	–
120	188	308	6.966	6.965	6.961	–	–	–
120	190	310	6.956	6.950	6.945	–	–	–
122	170	292	6.897	6.925	6.927	–	–	–
122	172	294	6.909	6.936	6.937	–	–	–
122	174	296	6.919	6.943	6.944	–	–	–
122	176	298	6.928	6.950	6.950	–	–	–
122	178	300	6.935	6.955	6.955	–	–	–
122	180	302	6.939	6.957	6.957	–	–	–
122	182	304	6.942	6.958	6.957	–	–	–
122	184	306	6.942	6.957	6.955	–	–	–
122	186	308	6.937	6.934	6.944	–	–	–
122	188	310	6.929	6.934	6.931	–	–	–
122	190	312	6.921	6.922	6.918	–	–	–
124	170	294	6.830	6.864	6.867	–	–	–
124	172	296	6.845	6.876	6.879	–	–	–
124	174	298	6.859	6.888	6.889	–	–	–
124	176	300	6.870	6.898	6.899	–	–	–
124	178	302	6.879	6.906	6.906	–	–	–
124	180	304	6.888	6.911	6.911	–	–	–
124	182	306	6.893	6.914	6.915	–	–	–
124	184	308	6.896	6.916	6.915	–	–	–
124	186	310	6.892	6.908	6.906	–	–	–
124	188	312	6.887	6.898	6.896	–	–	–
124	190	314	6.881	6.888	6.885	–	–	–
126	170	296	6.760	6.798	6.801	–	–	–
126	172	298	6.777	6.813	6.816	–	–	–
126	174	300	6.793	6.827	6.829	–	–	–
126	176	302	6.807	6.839	6.841	–	–	–

Table 4 – *Continued on next page*

Table 4 – Continued from previous page

Z	N	A	BE/A					
			SkM*	SLy5	SLy4	SkM*	SLy5	SLy4
			(HFB)	(HFB)	(HFB)			
126	178	304	6.819	6.850	6.851	–	–	–
126	180	306	6.830	6.858	6.859	–	–	–
126	182	308	6.838	6.865	6.865	–	–	–
126	184	310	6.843	6.869	6.869	–	–	–
126	186	312	6.842	6.863	6.862	–	–	–
126	188	314	6.839	6.856	6.854	–	–	–
126	190	316	6.835	6.843	6.845	–	–	–
128	170	298	6.686	6.728	6.732	–	–	–
128	172	300	6.706	6.746	6.749	–	–	–
128	174	302	6.723	6.762	6.765	–	–	–
128	176	304	6.738	6.776	6.779	–	–	–
128	178	306	6.753	6.788	6.791	–	–	–
128	180	308	6.765	6.799	6.800	–	–	–
128	182	310	6.776	6.808	6.808	–	–	–
128	184	312	6.783	6.814	6.814	–	–	–
128	186	314	6.784	6.811	6.810	–	–	–
128	188	316	6.783	6.807	6.805	–	–	–
128	190	318	6.782	6.800	6.799	–	–	–
130	170	300	6.609	6.655	6.659	–	–	–
130	172	302	6.631	6.675	6.679	–	–	–
130	174	304	6.650	6.693	6.696	–	–	–
130	176	306	6.667	6.709	6.712	–	–	–
130	178	308	6.683	6.724	6.726	–	–	–
130	180	310	6.697	6.736	6.738	–	–	–
130	182	312	6.710	6.747	6.748	–	–	–
130	184	314	6.719	6.755	6.756	–	–	–
130	186	316	6.722	6.755	6.755	–	–	–
130	188	318	6.727	6.753	6.752	–	–	–
130	190	320	6.732	6.753	6.751	–	–	–

Table 5: Calculated root-mean-square radius r_{rms} for Skyrme parameters of SkM*, SLy5, and SLy4.

Z	N	A	r_{rms}					
			SkM*	SLy5	SLy4	SkM*	SLy5	SLy4
			(HFB)	(HFB)	(HFB)			
112	170	282	6.223	6.206	6.214	—	—	—
112	172	284	6.214	6.213	6.220	—	—	—
112	174	286	6.224	6.224	6.231	—	—	—
112	176	288	6.233	6.228	6.234	—	—	—
112	178	290	6.245	6.236	6.241	—	—	—
112	180	292	6.254	6.245	6.251	—	—	—
112	182	294	6.265	6.256	6.262	—	—	—
112	184	296	6.278	6.267	6.273	—	—	—
112	186	298	6.296	6.287	6.293	—	—	—
112	188	300	6.314	6.307	6.312	—	—	—
112	190	302	6.331	6.326	6.331	—	—	—
114	170	284	6.231	6.217	6.226	—	—	—
114	172	286	6.224	6.224	6.231	—	—	—
114	174	288	6.233	6.235	6.243	—	—	—
114	176	290	6.243	6.239	6.245	—	—	—
114	178	292	6.255	6.246	6.253	—	—	—
114	180	294	6.264	6.255	6.261	—	—	—
114	182	296	6.275	6.265	6.272	—	—	—
114	184	298	6.287	6.277	6.283	—	—	—
114	186	300	6.306	6.297	6.303	—	—	—
114	188	302	6.323	6.316	6.322	—	—	—
114	190	304	6.340	6.335	6.340	—	—	—
116	170	286	6.221	6.228	6.238	—	—	—
116	172	288	6.233	6.234	6.241	—	—	—
116	174	290	6.243	6.245	6.253	—	—	—
116	176	292	6.253	6.246	6.254	—	—	—
116	178	294	6.265	6.256	6.263	—	—	—
116	180	296	6.274	6.265	6.272	—	—	—
116	182	298	6.285	6.275	6.282	—	—	—
116	184	300	6.297	6.287	6.293	—	—	—
116	186	302	6.315	6.307	6.313	—	—	—
116	188	304	6.332	6.326	6.332	—	—	—
116	190	306	6.349	6.345	6.350	—	—	—
118	170	288	6.229	6.231	6.238	—	—	—

Table 5 – *Continued on next page*

Table 5 – Continued from previous page

Z	N	A	r_{rms}					
			SkM*	SLy5	SLy4	SkM* (HFB)	SLy5 (HFB)	SLy4 (HFB)
118	172	290	6.242	6.241	6.248	–	–	–
118	174	292	6.253	6.253	6.253	–	–	–
118	176	294	6.264	6.257	6.263	–	–	–
118	178	296	6.275	6.267	6.273	–	–	–
118	180	298	6.284	6.275	6.282	–	–	–
118	182	300	6.295	6.286	6.293	–	–	–
118	184	302	6.307	6.297	6.303	–	–	–
118	186	304	6.325	6.317	6.323	–	–	–
118	188	306	6.342	6.336	6.341	–	–	–
118	190	308	6.358	6.354	6.359	–	–	–
120	170	290	6.240	6.237	6.243	6.233	6.229	6.235
120	172	292	6.252	6.248	6.255	6.246	6.242	6.250
120	174	294	6.264	6.257	6.264	6.254	6.252	6.260
120	176	296	6.274	6.267	6.274	6.267	6.262	6.271
120	178	298	6.285	6.277	6.283	6.279	6.271	6.279
120	180	300	6.294	6.285	6.291	6.290	6.279	6.288
120	182	302	6.305	6.296	6.303	–	–	–
120	184	304	6.316	6.306	6.313	–	–	–
120	186	306	6.334	6.335	6.332	–	–	–
120	188	308	6.351	6.345	6.351	–	–	–
120	190	310	6.367	6.363	6.369	–	–	–
122	170	292	6.260	6.259	6.268	–	–	–
122	172	294	6.269	6.271	6.278	–	–	–
122	174	296	6.271	6.267	6.274	–	–	–
122	176	298	6.282	6.276	6.283	–	–	–
122	178	300	6.293	6.286	6.293	–	–	–
122	180	302	6.302	6.295	6.302	–	–	–
122	182	304	6.314	6.305	6.312	–	–	–
122	184	306	6.326	6.316	6.322	–	–	–
122	186	308	6.343	6.326	6.341	–	–	–
122	188	310	6.359	6.353	6.359	–	–	–
122	190	312	6.375	6.371	6.377	–	–	–
124	170	294	6.277	6.276	6.283	–	–	–
124	172	296	6.266	6.280	6.293	–	–	–
124	174	298	6.278	6.275	6.281	–	–	–
124	176	300	6.290	6.285	6.291	–	–	–

Table 5 – Continued on next page

Table 5 – *Continued from previous page*

Z	N	A	r_{rms}					
			SkM*	SLy5	SLy4	SkM*	SLy5	SLy4
			(HFB)	(HFB)	(HFB)			
124	178	302	6.298	6.294	6.301	–	–	–
124	180	304	6.310	6.303	6.310	–	–	–
124	182	306	6.322	6.314	6.321	–	–	–
124	184	308	6.334	6.324	6.331	–	–	–
124	186	310	6.351	6.344	6.350	–	–	–
124	188	312	6.367	6.362	6.368	–	–	–
124	190	314	6.383	6.379	6.385	–	–	–
126	170	296	6.294	6.288	6.296	–	–	–
126	172	298	6.297	6.290	6.304	–	–	–
126	174	300	6.301	6.296	6.304	–	–	–
126	176	302	6.298	6.306	6.313	–	–	–
126	178	304	6.310	6.303	6.322	–	–	–
126	180	306	6.322	6.314	6.320	–	–	–
126	182	308	6.334	6.324	6.331	–	–	–
126	184	310	6.345	6.335	6.342	–	–	–
126	186	312	6.362	6.354	6.361	–	–	–
126	188	314	6.378	6.372	6.379	–	–	–
126	190	316	6.394	6.474	6.396	–	–	–
128	170	298	6.313	6.305	6.313	–	–	–
128	172	300	6.321	6.311	6.321	–	–	–
128	174	302	6.324	6.317	6.324	–	–	–
128	176	304	6.318	6.326	6.333	–	–	–
128	178	306	6.329	6.322	6.342	–	–	–
128	180	308	6.341	6.332	6.339	–	–	–
128	182	310	6.353	6.343	6.350	–	–	–
128	184	312	6.364	6.353	6.361	–	–	–
128	186	314	6.381	6.372	6.379	–	–	–
128	188	316	6.396	6.390	6.397	–	–	–
128	190	318	6.412	6.495	6.414	–	–	–
130	170	300	6.333	6.325	6.327	–	–	–
130	172	302	6.342	6.332	6.337	–	–	–
130	174	304	6.346	6.337	6.345	–	–	–
130	176	306	6.354	6.345	6.352	–	–	–
130	178	308	6.348	6.352	6.360	–	–	–
130	180	310	6.359	6.351	6.358	–	–	–
130	182	312	6.371	6.361	6.368	–	–	–

Table 5 – *Continued on next page*

Deformed magic numbers at $N = 178$ and $Z = 120, 124$ in superheavy region 29

Table 5 – Continued from previous page

Z	N	A	r_{rms}					
			SkM*	SLy5	SLy4	SkM*	SLy5	SLy4
			(HFB)	(HFB)	(HFB)			
130	184	314	6.382	6.371	6.378	–	–	–
130	186	316	6.398	6.390	6.397	–	–	–
130	188	318	6.520	6.408	6.415	–	–	–
130	190	320	6.532	6.521	6.523	–	–	–

Table 6: Calculated charge radius r_p for Skyrme parameters of SkM*, SLy5, and SLy4

Z	N	A	r_p					
			SkM*	SLy5	SLy4	SkM*	SLy5	SLy4
			(HFB)	(HFB)	(HFB)			
112	170	282	6.151	6.135	6.145	–	–	–
112	172	284	6.138	6.138	6.147	–	–	–
112	174	286	6.142	6.145	6.153	–	–	–
112	176	288	6.146	6.144	6.152	–	–	–
112	178	290	6.152	6.146	6.153	–	–	–
112	180	292	6.156	6.149	6.157	–	–	–
112	182	294	6.160	6.154	6.162	–	–	–
112	184	296	6.166	6.159	6.167	–	–	–
112	186	298	6.179	6.173	6.181	–	–	–
112	188	300	6.190	6.187	6.194	–	–	–
112	190	302	6.201	6.201	6.331	–	–	–
114	170	284	6.166	6.154	6.165	–	–	–
114	172	286	6.156	6.157	6.166	–	–	–
114	174	288	6.160	6.164	6.173	–	–	–
114	176	290	6.164	6.162	6.170	–	–	–
114	178	292	6.171	6.164	6.173	–	–	–
114	180	294	6.175	6.168	6.176	–	–	–
114	182	296	6.180	6.172	6.182	–	–	–
114	184	298	6.185	6.178	6.187	–	–	–
114	186	300	6.198	6.193	6.200	–	–	–
114	188	302	6.209	6.206	6.214	–	–	–
114	190	304	6.221	6.220	6.227	–	–	–
116	170	286	6.165	6.172	6.184	–	–	–

Table 6 – Continued on next page

Table 6 – *Continued from previous page*

<i>Z</i>	<i>N</i>	<i>A</i>	<i>r_p</i>					
			SkM*	SLy5	SLy4	SkM* (HFB)	SLy5 (HFB)	SLy4 (HFB)
116	172	288	6.173	6.174	6.183	–	–	–
116	174	290	6.178	6.181	6.190	–	–	–
116	176	292	6.183	6.177	6.187	–	–	–
116	178	294	6.189	6.183	6.191	–	–	–
116	180	296	6.193	6.186	6.194	–	–	–
116	182	298	6.198	6.191	6.200	–	–	–
116	184	300	6.204	6.197	6.205	–	–	–
116	186	302	6.217	6.211	6.219	–	–	–
116	188	304	6.228	6.225	6.233	–	–	–
116	190	306	6.239	6.238	6.246	–	–	–
118	170	288	6.181	6.182	6.190	–	–	–
118	172	290	6.189	6.187	6.196	–	–	–
118	174	292	6.195	6.195	6.197	–	–	–
118	176	294	6.200	6.195	6.203	–	–	–
118	178	296	6.207	6.200	6.209	–	–	–
118	180	298	6.211	6.204	6.212	–	–	–
118	182	300	6.216	6.209	6.218	–	–	–
118	184	302	6.222	6.215	6.223	–	–	–
118	186	304	6.234	6.229	6.237	–	–	–
118	188	306	6.246	6.243	6.250	–	–	–
118	190	308	6.257	6.256	6.263	–	–	–
120	170	290	6.198	6.195	6.203	6.244	6.241	6.248
120	172	292	6.206	6.201	6.210	6.252	6.248	6.257
120	174	294	6.212	6.206	6.214	6.259	6.254	6.263
120	176	296	6.218	6.212	6.220	6.267	6.259	6.269
120	178	298	6.224	6.217	6.225	6.280	6.267	6.276
120	180	300	6.228	6.221	6.228	6.278	6.269	6.280
120	182	302	6.233	6.226	6.235	–	–	–
120	184	304	6.239	6.232	6.240	–	–	–
120	186	306	6.251	6.261	6.254	–	–	–
120	188	308	6.262	6.259	6.267	–	–	–
120	190	310	6.273	6.272	6.280	–	–	–
122	170	292	6.227	6.226	6.236	–	–	–
122	172	294	6.230	6.233	6.242	–	–	–
122	174	296	6.226	6.222	6.230	–	–	–
122	176	298	6.232	6.227	6.235	–	–	–

Table 6 – *Continued on next page*

Deformed magic numbers at $N = 178$ and $Z = 120, 124$ in superheavy region 31

Table 6 – Continued from previous page

Z	N	A	r_p			
			SkM*	SLy5	SLy4	SkM* (HFB)
122	178	300	6.239	6.233	6.241	–
122	180	302	6.242	6.236	6.245	–
122	182	304	6.249	6.242	6.251	–
122	184	306	6.255	6.247	6.256	–
122	186	308	6.267	6.246	6.269	–
122	188	310	6.278	6.275	6.282	–
122	190	312	6.288	6.288	6.295	–
124	170	294	6.252	6.250	6.258	–
124	172	296	6.232	6.249	6.264	–
124	174	298	6.239	6.236	6.243	–
124	176	300	6.245	6.241	6.249	–
124	178	302	6.249	6.246	6.254	–
124	180	304	6.256	6.250	6.259	–
124	182	306	6.264	6.256	6.265	–
124	184	308	6.270	6.262	6.271	–
124	186	310	6.282	6.276	6.284	–
124	188	312	6.292	6.289	6.297	–
124	190	314	6.303	6.302	6.309	–
126	170	296	6.276	6.269	6.278	–
126	172	298	6.272	6.265	6.281	–
126	174	300	6.271	6.266	6.275	–
126	176	302	6.261	6.271	6.279	–
126	178	304	6.268	6.261	6.285	–
126	180	306	6.275	6.267	6.275	–
126	182	308	6.282	6.273	6.281	–
126	184	310	6.288	6.279	6.287	–
126	186	312	6.299	6.293	6.301	–
126	188	314	6.310	6.306	6.314	–
126	190	316	6.321	6.414	6.327	–
128	170	298	6.304	6.293	6.301	–
128	172	300	6.307	6.293	6.305	–
128	174	302	6.303	6.295	6.303	–
128	176	304	6.289	6.299	6.307	–
128	178	306	6.296	6.288	6.313	–
128	180	308	6.303	6.294	6.303	–
128	182	310	6.310	6.300	6.309	–

Table 6 – Continued on next page

Table 6 – *Continued from previous page*

Z	N	A	r_p					
			SkM*	SLy5	SLy4	SkM*	SLy5	SLy4
			(HFB)	(HFB)	(HFB)			
128	184	312	6.316	6.306	6.315	–	–	–
128	186	314	6.328	6.320	6.329	–	–	–
128	188	316	6.338	6.333	6.341	–	–	–
128	190	318	6.349	6.443	6.354	–	–	–
130	170	300	6.331	6.320	6.322	–	–	–
130	172	302	6.336	6.323	6.329	–	–	–
130	174	304	6.333	6.323	6.332	–	–	–
130	176	306	6.337	6.326	6.334	–	–	–
130	178	308	6.324	6.330	6.338	–	–	–
130	180	310	6.330	6.321	6.330	–	–	–
130	182	312	6.337	6.327	6.336	–	–	–
130	184	314	6.343	6.332	6.342	–	–	–
130	186	316	6.355	6.347	6.355	–	–	–
130	188	318	6.481	6.360	6.368	–	–	–
130	190	320	6.488	6.477	6.480	–	–	–

Table 7: Calculated Q_α -values (MeV) with Skyrme parametrization SkM* (Q_{SkM^*}), SLy5 (Q_{SLy5}) and SLy4 (Q_{SLy4}) with the averaged of all Madland’s pairing strength, and experimental Q_α -value ($Q_\alpha^{exp.}$) are taken from⁴ and⁷⁵.

Z	N	A	$Q_{SkM^*}^{Ave}$	Q_{SLy5}^{Ave}	Q_{SLy4}^{Ave}	$Q_\alpha^{exp.}$
114	172	286	11.36	10.14	10.16	10.35
114	174	288	10.54	9.70	9.68	10.07
114	176	290	10.14	10.27	9.81	9.86
114	178	292	9.85	8.59	8.57	–
114	180	294	9.98	9.24	8.31	–
114	182	296	9.33	8.57	8.34	–
114	184	298	9.37	8.49	8.48	–
114	186	300	10.77	10.51	10.66	–
114	188	302	10.71	10.27	10.39	–
114	190	304	10.47	9.93	10.05	–
116	172	288	11.62	10.99	11.02	–
116	174	290	11.26	10.58	10.56	11.00

Table 7 – *Continued on next page*

Table 7 – Continued from previous page

Z	N	A	$Q_{SkM^*}^{Ave}$	Q_{SLy5}^{Ave}	Q_{SLy4}^{Ave}	$Q_\alpha^{exp.}$
116	176	292	10.89	11.08	10.75	10.78
116	178	294	10.66	9.40	9.41	—
116	180	296	10.81	9.99	10.07	—
116	182	298	10.35	9.26	9.14	—
116	184	300	10.58	9.04	9.26	—
116	186	302	11.87	11.27	11.42	—
116	188	304	11.82	11.04	11.16	—
116	190	306	11.57	10.72	10.84	—
118	172	290	11.98	11.96	12.01	—
118	174	292	12.12	11.59	11.91	—
118	176	294	11.80	11.69	11.33	11.82
118	178	296	11.63	10.24	10.14	—
118	180	298	11.89	10.84	10.90	—
118	182	300	11.51	10.20	10.08	—
118	184	302	11.67	10.15	10.23	—
118	186	304	12.88	12.31	12.43	—
118	188	306	12.83	12.08	12.18	—
118	190	308	12.59	11.77	11.87	—
120	172	292	13.08	12.92	12.55	—
120	174	294	13.20	12.69	12.35	—
120	176	296	13.00	12.26	11.54	—
120	178	298	12.85	11.36	11.28	—
120	180	300	13.04	11.92	11.96	—
120	182	302	12.56	11.33	11.14	—
120	184	304	12.64	11.24	11.30	—
120	186	306	13.82	13.37	13.47	—
120	188	308	13.78	13.14	13.21	—
120	190	310	13.55	12.83	12.91	—
122	172	294	14.87	13.58	13.29	—
122	174	296	14.82	13.70	13.71	—
122	176	298	14.39	13.21	13.16	—
122	178	300	14.09	12.88	12.78	—
122	180	302	14.12	13.02	13.06	—
122	182	304	13.53	12.51	12.21	—
122	184	306	13.59	12.25	12.35	—
122	186	308	14.80	14.43	14.50	—
122	188	310	14.78	14.20	14.25	—
122	190	312	14.55	13.91	13.94	—

Table 7 – Continued on next page

Table 7 – *Continued from previous page*

Z	N	A	$Q_{SkM^*}^{Ave}$	Q_{SLy5}^{Ave}	Q_{SLy4}^{Ave}	$Q_\alpha^{exp.}$
124	172	296	15.85	15.05	14.86	—
124	174	298	15.55	14.81	14.94	—
124	176	300	15.19	14.08	14.01	—
124	178	302	15.19	13.88	13.81	—
124	180	304	14.86	13.88	13.87	—
124	182	306	14.44	13.64	13.35	—
124	184	308	14.66	13.23	13.43	—
124	186	310	15.92	15.58	15.65	—
124	188	312	15.91	15.37	15.41	—
124	190	314	15.71	15.09	15.12	—
126	172	298	16.80	15.93	15.80	—
126	174	300	16.72	15.61	15.78	—
126	176	302	16.56	15.37	15.28	—
126	178	304	16.33	15.31	15.27	—
126	180	306	15.96	15.20	15.22	—
126	182	308	16.06	14.95	14.99	—
126	184	310	16.27	14.61	14.84	—
126	186	312	17.61	17.12	17.25	—
126	188	314	17.59	16.89	17.00	—
126	190	316	17.38	16.60	16.70	—
128	172	300	17.59	16.73	16.59	—
128	174	302	17.65	16.59	16.63	—
128	176	304	17.72	16.43	16.33	—
128	178	306	17.56	16.53	16.28	—
128	180	308	17.64	16.45	16.45	—
128	182	310	17.80	16.49	16.49	—
128	184	312	18.14	16.54	16.52	—
128	186	314	19.47	19.03	19.14	—
128	188	316	19.34	18.66	18.78	—
128	190	318	19.06	18.24	18.36	—
130	172	302	18.28	17.52	17.38	—
130	174	304	18.52	17.51	17.53	—
130	176	306	18.45	17.37	17.30	—
130	178	308	18.39	17.37	17.25	—
130	180	310	18.49	17.38	17.56	—
130	182	312	18.67	17.45	17.40	—
130	184	314	19.07	17.55	17.45	—
130	186	316	20.24	19.80	19.88	—

Table 7 – *Continued on next page*

Table 7 – Continued from previous page

Z	N	A	$Q_{SkM^*}^{Ave}$	Q_{SLy5}^{Ave}	Q_{SLy4}^{Ave}	$Q_\alpha^{exp.}$
130	188	318	19.15	19.45	19.53	–
130	190	320	17.58	18.28	18.43	–

Table 8: Comparison of calculated logarithmic α -decay half-lives with Skyrme SkM* Skyrme parametrization $\log T_{1/2}^{SkM^*}$ (s) together with experimental half-lives $\log T_{1/2}^{exp.}$ (s) taken from⁴ and⁷⁵.

Z	N	A	$T_{1/2}^{VSS1}$	$T_{1/2}^{VSS2}$	$T_{1/2}^{PS}$	$T_{1/2}^R$	$T_{1/2}^{mR}$	$T_{1/2}^{BF}$	$T_{1/2}^{MB1}$	$T_{1/2}^{MB2}$	$T_{1/2}^{exp.}$
114	172	286	-3.29	-2.74	-2.90	-3.53	-3.48	-3.36	-3.17	-3.37	-0.92
114	174	288	-1.24	-0.79	-0.92	-1.51	-1.47	-1.52	-1.46	-1.32	-0.18
114	176	290	-0.15	0.25	0.14	-0.46	-0.42	-0.55	-0.55	-0.24	1.90
114	178	292	0.67	1.03	0.93	0.32	0.36	0.19	0.13	0.59	–
114	180	294	0.30	0.68	0.58	-0.08	-0.04	-0.14	-0.17	0.22	–
114	182	296	2.27	2.55	2.48	1.85	1.88	1.62	1.46	2.18	–
114	184	298	2.14	2.43	2.36	1.69	1.72	1.50	1.36	2.06	–
114	186	300	-1.85	-1.37	-1.50	-2.34	-2.29	-2.06	-1.96	-1.93	–
114	188	302	-1.70	-1.22	-1.36	-2.22	-2.18	-1.93	-1.84	-1.78	–
114	190	304	-1.06	-0.62	-0.74	-1.62	-1.58	-1.36	-1.31	-1.14	–
116	172	288	-3.32	-2.71	-2.90	-3.51	-3.47	-3.39	-3.26	-3.41	–
116	174	290	-2.46	-1.90	-2.07	-2.69	-2.65	-2.62	-2.55	-2.56	-2.08
116	176	292	-1.54	-1.02	-1.18	-1.81	-1.76	-1.81	-1.79	-1.64	-1.89
116	178	294	-0.93	-0.44	-0.59	-1.23	-1.19	-1.26	-1.29	-1.04	–
116	180	296	-1.33	-0.82	-0.98	-1.67	-1.63	-1.62	-1.62	-1.43	–
116	182	298	-0.09	0.35	0.22	-0.47	-0.43	-0.52	-0.59	-0.20	–
116	184	300	-0.73	-0.26	-0.40	-1.15	-1.10	-1.09	-1.13	-0.84	–
116	186	302	-3.90	-3.26	-3.46	-4.35	-4.30	-3.90	-3.74	-3.98	–
116	188	304	-3.78	-3.15	-3.34	-4.26	-4.21	-3.79	-3.64	-3.86	–
116	190	306	-3.21	-2.61	-2.79	-3.73	-3.68	-3.29	-3.17	-3.30	–
118	172	290	-3.59	-2.91	-3.14	-3.73	-3.69	-3.62	-3.54	-3.67	–
118	174	292	-3.90	-3.20	-3.43	-4.07	-4.03	-3.89	-3.79	-3.97	–
118	176	294	-3.17	-2.51	-2.73	-3.39	-3.34	-3.25	-3.20	-3.26	-3.16
118	178	296	-2.77	-2.13	-2.34	-3.02	-2.98	-2.90	-2.87	-2.87	–
118	180	298	-3.37	-2.70	-2.92	-3.66	-3.61	-3.43	-3.36	-3.46	–
118	182	300	-2.49	-1.87	-2.07	-2.82	-2.78	-2.66	-2.65	-2.60	–
118	184	302	-2.86	-2.22	-2.43	-3.23	-3.18	-2.98	-2.95	-2.96	–
118	186	304	-5.51	-4.73	-4.99	-5.90	-5.85	-5.31	-5.12	-5.56	–

Table 8 – Continued on next page

Table 8 – *Continued from previous page*

Z	N	A	$T_{1/2}^{VSS1}$	$T_{1/2}^{VSS2}$	$T_{1/2}^{PS}$	$T_{1/2}^R$	$T_{1/2}^{mR}$	$T_{1/2}^{BF}$	$T_{1/2}^{MB1}$	$T_{1/2}^{MB2}$	$T_{1/2}^{exp.}$
118	188	306	-5.42	-4.65	-4.90	-5.85	-5.80	-5.23	-5.04	-5.47	—
118	190	308	-4.90	-4.16	-4.40	-5.37	-5.32	-4.78	-4.62	-4.97	—
120	172	292	-5.41	-4.57	-4.86	-5.49	-5.45	-5.21	-5.08	-5.45	—
120	174	294	-5.64	-4.79	-5.09	-5.76	-5.71	-5.41	-5.26	-5.67	—
120	176	296	-5.23	-4.41	-4.69	-5.40	-5.35	-5.06	-4.94	-5.28	—
120	178	298	-4.92	-4.11	-4.39	-5.12	-5.07	-4.78	-4.68	-4.97	—
120	180	300	-5.31	-4.48	-4.77	-5.55	-5.50	-5.12	-5.00	-5.35	—
120	182	302	-4.32	-3.55	-3.81	-4.60	-4.55	-4.26	-4.20	-4.39	—
120	184	304	-4.48	-3.69	-3.96	-4.79	-4.74	-4.39	-4.32	-4.54	—
120	186	306	-6.83	-5.92	-6.24	-7.17	-7.12	-6.45	-6.23	-6.83	—
120	188	308	-6.76	-5.85	-6.17	-7.14	-7.09	-6.39	-6.18	-6.77	—
120	190	310	-6.32	-5.43	-5.74	-6.73	-6.68	-6.00	-5.81	-6.33	—
122	172	294	-8.22	-7.16	-7.54	-8.24	-8.19	-7.63	-7.38	-8.15	—
122	174	296	-8.14	-7.09	-7.47	-8.20	-8.15	-7.56	-7.31	-8.07	—
122	176	298	-7.39	-6.38	-6.74	-7.49	-7.43	-6.90	-6.71	-7.34	—
122	178	300	-6.85	-5.87	-6.22	-6.99	-6.94	-6.44	-6.28	-6.82	—
122	180	302	-6.90	-5.91	-6.27	-7.07	-7.02	-6.48	-6.31	-6.87	—
122	182	304	-5.78	-4.86	-5.19	-6.00	-5.95	-5.51	-5.41	-5.79	—
122	184	306	-5.91	-4.98	-5.31	-6.16	-6.11	-5.62	-5.52	-5.91	—
122	186	308	-8.09	-7.04	-7.42	-8.37	-8.32	-7.52	-7.28	-8.03	—
122	188	310	-8.06	-7.01	-7.39	-8.38	-8.32	-7.49	-7.25	-8.00	—
122	190	312	-7.67	-6.64	-7.01	-8.02	-7.97	-7.15	-6.93	-7.62	—
124	172	296	-9.38	-8.18	-8.63	-9.34	-9.28	-8.59	-8.32	-9.22	—
124	174	298	-8.90	-7.73	-8.17	-8.90	-8.84	-8.17	-7.94	-8.76	—
124	176	300	-8.30	-7.16	-7.59	-8.34	-8.28	-7.65	-7.46	-8.18	—
124	178	302	-8.30	-7.17	-7.59	-8.38	-8.32	-7.66	-7.46	-8.19	—
124	180	304	-7.74	-6.64	-7.05	-7.86	-7.80	-7.17	-7.01	-7.65	—
124	182	306	-7.01	-5.95	-6.34	-7.16	-7.11	-6.54	-6.42	-6.94	—
124	184	308	-7.39	-6.31	-6.71	-7.58	-7.53	-6.87	-6.73	-7.31	—
124	186	310	-9.49	-8.28	-8.73	-9.70	-9.65	-8.68	-8.40	-9.33	—
124	188	312	-9.46	-8.26	-8.71	-9.71	-9.66	-8.66	-8.38	-9.30	—
124	190	314	-9.15	-7.96	-8.41	-9.44	-9.38	-8.39	-8.13	-9.00	—
126	172	298	-10.39	-9.06	-9.57	-10.28	-10.22	-9.40	-9.12	-10.14	—
126	174	300	-10.28	-8.95	-9.46	-10.21	-10.15	-9.30	-9.03	-10.03	—
126	176	302	-10.04	-8.73	-9.23	-10.01	-9.95	-9.10	-8.85	-9.80	—
126	178	304	-9.69	-8.40	-8.90	-9.70	-9.64	-8.80	-8.57	-9.47	—
126	180	306	-9.12	-7.86	-8.34	-9.17	-9.11	-8.31	-8.12	-8.92	—
126	182	308	-9.27	-8.00	-8.49	-9.35	-9.29	-8.44	-8.24	-9.06	—

Table 8 – *Continued on next page*

Table 8 – Continued from previous page

Z	N	A	$T_{1/2}^{VSS1}$	$T_{1/2}^{VSS2}$	$T_{1/2}^{PS}$	$T_{1/2}^R$	$T_{1/2}^{mR}$	$T_{1/2}^{BF}$	$T_{1/2}^{MB1}$	$T_{1/2}^{MB2}$	$T_{1/2}^{exp.}$
126	184	310	-9.59	-8.31	-8.80	-9.71	-9.65	-8.72	-8.49	-9.37	–
126	186	312	-11.53	-10.13	-10.67	-11.68	-11.61	-10.38	-10.02	-11.23	–
126	188	314	-11.50	-10.10	-10.64	-11.68	-11.62	-10.35	-10.00	-11.20	–
126	190	316	-11.22	-9.83	-10.36	-11.43	-11.37	-10.11	-9.78	-10.92	–
128	172	300	-11.12	-9.66	-10.23	-10.94	-10.88	-9.96	-9.69	-10.76	–
128	174	302	-11.20	-9.73	-10.31	-11.05	-10.99	-10.03	-9.75	-10.84	–
128	176	304	-11.29	-9.82	-10.39	-11.18	-11.12	-10.10	-9.82	-10.92	–
128	178	306	-11.07	-9.61	-10.18	-11.00	-10.94	-9.92	-9.65	-10.72	–
128	180	308	-11.18	-9.72	-10.29	-11.15	-11.09	-10.01	-9.74	-10.82	–
128	182	310	-11.40	-9.93	-10.51	-11.41	-11.35	-10.20	-9.91	-11.03	–
128	184	312	-11.86	-10.35	-10.95	-11.90	-11.84	-10.59	-10.27	-11.47	–
128	186	314	-13.52	-11.91	-12.55	-13.59	-13.52	-12.00	-11.57	-13.04	–
128	188	316	-13.37	-11.78	-12.41	-13.48	-13.42	-11.88	-11.46	-12.90	–
128	190	318	-13.03	-11.45	-12.07	-13.17	-13.10	-11.58	-11.19	-12.57	–
130	172	302	-11.67	-10.10	-10.73	-11.42	-11.36	-10.36	-10.11	-11.21	–
130	174	304	-11.99	-10.39	-11.03	-11.77	-11.71	-10.63	-10.36	-11.51	–
130	176	306	-11.89	-10.30	-10.94	-11.71	-11.65	-10.55	-10.28	-11.42	–
130	178	308	-11.82	-10.24	-10.87	-11.68	-11.62	-10.49	-10.22	-11.35	–
130	180	310	-11.94	-10.35	-10.99	-11.84	-11.78	-10.59	-10.32	-11.47	–
130	182	312	-12.18	-10.57	-11.22	-12.11	-12.05	-10.79	-10.50	-11.69	–
130	184	314	-12.69	-11.05	-11.71	-12.66	-12.59	-11.22	-10.90	-12.17	–
130	186	316	-14.08	-12.36	-13.05	-14.08	-14.01	-12.40	-11.98	-13.49	–
130	188	318	-12.78	-11.14	-11.80	-12.82	-12.76	-11.30	-10.97	-12.26	–
130	190	320	-10.71	-9.20	-9.80	-10.80	-10.74	-9.55	-9.36	-10.31	–

Table 9: Comparison of calculated logarithmic α -decay half-lives with Skyrme SLy5 parametrization $\log T_{1/2}^{SLy5}$ (s) together with experimental half-lives $\log T_{1/2}^{exp.}$ (s) taken from⁴ and⁷⁵.

Z	N	A	$T_{1/2}^{VSS1}$	$T_{1/2}^{VSS2}$	$T_{1/2}^{PS}$	$T_{1/2}^R$	$T_{1/2}^{mR}$	$T_{1/2}^{BF}$	$T_{1/2}^{MB1}$	$T_{1/2}^{MB2}$	$T_{1/2}^{exp.}$
114	172	286	-0.15	0.25	0.14	-0.38	-0.34	-0.54	-0.55	-0.23	-0.92
114	174	288	1.13	1.47	1.38	0.85	0.89	0.60	0.51	1.04	-0.18
114	176	290	-0.51	-0.09	-0.21	-0.82	-0.78	-0.87	-0.85	-0.59	1.90
114	178	292	4.77	4.93	4.90	4.42	4.45	3.85	3.54	4.68	–
114	180	294	2.54	2.81	2.75	2.16	2.20	1.86	1.69	2.46	–

Table 9 – Continued on next page

Table 9 – *Continued from previous page*

Z	N	A	$T_{1/2}^{VSS1}$	$T_{1/2}^{VSS2}$	$T_{1/2}^{PS}$	$T_{1/2}^R$	$T_{1/2}^{mR}$	$T_{1/2}^{BF}$	$T_{1/2}^{MB1}$	$T_{1/2}^{MB2}$	$T_{1/2}^{exp.}$
114	182	296	4.82	4.98	4.96	4.40	4.44	3.90	3.59	4.73	–
114	184	298	5.12	5.26	5.24	4.66	4.69	4.16	3.84	5.03	–
114	186	300	-1.17	-0.72	-0.84	-1.66	-1.61	-1.46	-1.40	-1.25	–
114	188	302	-0.50	-0.09	-0.20	-1.03	-0.99	-0.86	-0.85	-0.59	–
114	190	304	0.46	0.83	0.73	-0.10	-0.06	0.00	-0.04	0.37	–
116	172	288	-1.79	-1.26	-1.42	-1.98	-1.94	-2.03	-2.00	-1.89	–
116	174	290	-0.72	-0.25	-0.39	-0.95	-0.91	-1.08	-1.12	-0.83	-2.08
116	176	292	-2.03	-1.49	-1.65	-2.30	-2.25	-2.24	-2.19	-2.13	-1.89
116	178	294	2.74	3.04	2.96	2.43	2.47	1.99	1.74	2.60	–
116	180	296	0.92	1.32	1.21	0.58	0.62	0.38	0.24	0.80	–
116	182	298	3.18	3.46	3.39	2.80	2.84	2.38	2.11	3.04	–
116	184	300	3.91	4.16	4.10	3.50	3.53	3.04	2.71	3.76	–
116	186	302	-2.49	-1.93	-2.10	-2.94	-2.90	-2.65	-2.58	-2.59	–
116	188	304	-1.92	-1.38	-1.54	-2.40	-2.35	-2.14	-2.10	-2.01	–
116	190	306	-1.10	-0.60	-0.75	-1.62	-1.57	-1.41	-1.43	-1.20	–
118	172	290	-3.54	-2.86	-3.08	-3.68	-3.63	-3.58	-3.50	-3.62	–
118	174	292	-2.67	-2.04	-2.25	-2.85	-2.81	-2.81	-2.79	-2.77	–
118	176	294	-2.93	-2.28	-2.49	-3.14	-3.10	-3.04	-3.00	-3.02	-3.16
118	178	296	0.84	1.29	1.15	0.58	0.62	0.28	0.08	0.69	–
118	180	298	-0.80	-0.27	-0.44	-1.10	-1.05	-1.17	-1.26	-0.93	–
118	182	300	0.96	1.40	1.27	0.63	0.67	0.39	0.18	0.81	–
118	184	302	1.10	1.53	1.40	0.73	0.77	0.51	0.29	0.94	–
118	186	304	-4.32	-3.60	-3.84	-4.71	-4.67	-4.26	-4.14	-4.39	–
118	188	306	-3.80	-3.12	-3.34	-4.24	-4.19	-3.81	-3.72	-3.89	–
118	190	308	-3.11	-2.46	-2.67	-3.58	-3.53	-3.20	-3.15	-3.20	–
120	172	292	-5.08	-4.26	-4.54	-5.17	-5.12	-4.92	-4.81	-5.12	–
120	174	294	-4.59	-3.80	-4.08	-4.72	-4.67	-4.50	-4.42	-4.65	–
120	176	296	-3.66	-2.92	-3.17	-3.82	-3.78	-3.68	-3.66	-3.74	–
120	178	298	-1.54	-0.92	-1.13	-1.75	-1.71	-1.83	-1.94	-1.67	–
120	180	300	-2.88	-2.18	-2.42	-3.12	-3.07	-2.99	-3.02	-2.98	–
120	182	302	-1.48	-0.86	-1.06	-1.76	-1.72	-1.77	-1.89	-1.61	–
120	184	304	-1.24	-0.63	-0.84	-1.56	-1.52	-1.57	-1.70	-1.38	–
120	186	306	-5.97	-5.10	-5.40	-6.31	-6.26	-5.70	-5.53	-5.99	–
120	188	308	-5.51	-4.67	-4.96	-5.89	-5.84	-5.30	-5.16	-5.55	–
120	190	310	-4.88	-4.08	-4.36	-5.30	-5.25	-4.75	-4.65	-4.94	–
122	172	294	-5.88	-4.95	-5.28	-5.91	-5.86	-5.59	-5.49	-5.88	–
122	174	296	-6.12	-5.17	-5.51	-6.18	-6.13	-5.80	-5.68	-6.11	–

Table 9 – *Continued on next page*

Table 9 – Continued from previous page

Z	N	A	$T_{1/2}^{VSS1}$	$T_{1/2}^{VSS2}$	$T_{1/2}^{PS}$	$T_{1/2}^R$	$T_{1/2}^{mR}$	$T_{1/2}^{BF}$	$T_{1/2}^{MB1}$	$T_{1/2}^{MB2}$	$T_{1/2}^{exp.}$
122	176	298	-5.16	-4.27	-4.59	-5.26	-5.21	-4.97	-4.91	-5.18	–
122	178	300	-4.47	-3.62	-3.92	-4.61	-4.56	-4.37	-4.36	-4.51	–
122	180	302	-4.77	-3.90	-4.21	-4.95	-4.90	-4.63	-4.60	-4.80	–
122	182	304	-3.68	-2.88	-3.16	-3.90	-3.86	-3.69	-3.73	-3.75	–
122	184	306	-3.10	-2.33	-2.60	-3.36	-3.31	-3.18	-3.26	-3.19	–
122	186	308	-7.46	-6.44	-6.81	-7.74	-7.69	-6.96	-6.76	-7.41	–
122	188	310	-7.05	-6.06	-6.42	-7.37	-7.32	-6.61	-6.44	-7.02	–
122	190	312	-6.51	-5.55	-5.90	-6.87	-6.82	-6.15	-6.00	-6.50	–
124	172	296	-8.08	-6.95	-7.37	-8.04	-7.98	-7.46	-7.28	-7.97	–
124	174	298	-7.66	-6.56	-6.97	-7.66	-7.61	-7.11	-6.95	-7.57	–
124	176	300	-6.34	-5.32	-5.69	-6.38	-6.33	-5.96	-5.89	-6.30	–
124	178	302	-5.96	-4.96	-5.33	-6.05	-6.00	-5.64	-5.59	-5.94	–
124	180	304	-5.97	-4.97	-5.34	-6.09	-6.04	-5.65	-5.60	-5.94	–
124	182	306	-5.51	-4.53	-4.89	-5.67	-5.61	-5.25	-5.23	-5.50	–
124	184	308	-4.68	-3.76	-4.10	-4.88	-4.83	-4.54	-4.57	-4.70	–
124	186	310	-8.95	-7.77	-8.21	-9.17	-9.11	-8.21	-7.97	-8.81	–
124	188	312	-8.60	-7.44	-7.87	-8.85	-8.80	-7.91	-7.69	-8.47	–
124	190	314	-8.14	-7.01	-7.43	-8.43	-8.37	-7.51	-7.32	-8.03	–
126	172	298	-9.06	-7.81	-8.29	-8.96	-8.90	-8.26	-8.07	-8.87	–
126	174	300	-8.56	-7.33	-7.80	-8.49	-8.44	-7.83	-7.67	-8.38	–
126	176	302	-8.16	-6.96	-7.42	-8.14	-8.08	-7.49	-7.36	-8.00	–
126	178	304	-8.07	-6.87	-7.33	-8.08	-8.02	-7.41	-7.28	-7.91	–
126	180	306	-7.87	-6.68	-7.13	-7.92	-7.86	-7.24	-7.13	-7.72	–
126	182	308	-7.44	-6.28	-6.72	-7.53	-7.47	-6.87	-6.79	-7.31	–
126	184	310	-6.85	-5.72	-6.15	-6.98	-6.92	-6.37	-6.32	-6.75	–
126	186	312	-10.85	-9.49	-10.02	-11.00	-10.94	-9.80	-9.49	-10.58	–
126	188	314	-10.52	-9.18	-9.70	-10.71	-10.65	-9.52	-9.23	-10.26	–
126	190	316	-10.09	-8.78	-9.28	-10.32	-10.26	-9.15	-8.89	-9.85	–
128	172	300	-9.88	-8.50	-9.04	-9.71	-9.65	-8.91	-8.72	-9.59	–
128	174	302	-9.67	-8.30	-8.84	-9.54	-9.48	-8.73	-8.55	-9.39	–
128	176	304	-9.42	-8.07	-8.60	-9.33	-9.27	-8.52	-8.36	-9.15	–
128	178	306	-9.57	-8.21	-8.74	-9.51	-9.46	-8.65	-8.48	-9.30	–
128	180	308	-9.45	-8.10	-8.63	-9.43	-9.37	-8.54	-8.38	-9.18	–
128	182	310	-9.51	-8.15	-8.68	-9.53	-9.47	-8.59	-8.43	-9.24	–
128	184	312	-9.60	-8.23	-8.77	-9.65	-9.59	-8.67	-8.50	-9.32	–
128	186	314	-12.99	-11.42	-12.04	-13.06	-13.00	-11.55	-11.16	-12.54	–
128	188	316	-12.54	-10.99	-11.60	-12.64	-12.58	-11.17	-10.80	-12.11	–

Table 9 – Continued on next page

Table 9 – *Continued from previous page*

Z	N	A	$T_{1/2}^{VSS1}$	$T_{1/2}^{VSS2}$	$T_{1/2}^{PS}$	$T_{1/2}^R$	$T_{1/2}^{mR}$	$T_{1/2}^{BF}$	$T_{1/2}^{MB1}$	$T_{1/2}^{MB2}$	$T_{1/2}^{exp.}$
128	190	318	-11.99	-10.48	-11.07	-12.14	-12.08	-10.70	-10.37	-11.59	–
130	172	302	-10.63	-9.12	-9.72	-10.38	-10.32	-9.48	-9.30	-10.23	–
130	174	304	-10.62	-9.11	-9.71	-10.41	-10.35	-9.47	-9.29	-10.22	–
130	176	306	-10.41	-8.91	-9.51	-10.24	-10.18	-9.30	-9.13	-10.02	–
130	178	308	-10.41	-8.92	-9.52	-10.28	-10.22	-9.30	-9.13	-10.03	–
130	180	310	-10.43	-8.94	-9.53	-10.34	-10.28	-9.32	-9.14	-10.05	–
130	182	312	-10.53	-9.03	-9.63	-10.48	-10.42	-9.40	-9.22	-10.14	–
130	184	314	-10.67	-9.16	-9.76	-10.65	-10.59	-9.51	-9.33	-10.27	–
130	186	316	-13.57	-11.88	-12.56	-13.57	-13.50	-11.97	-11.59	-13.01	–
130	188	318	-13.15	-11.48	-12.15	-13.18	-13.12	-11.61	-11.26	-12.61	–
130	190	320	-11.67	-10.09	-10.73	-11.75	-11.69	-10.36	-10.11	-11.21	–

Table 10: Comparison of calculated logarithmic α -decay half-lives with Skyrme SLy4 Skyrme parametrization $\log T_{1/2}^{SLy4}$ (s) together with experimental half-lives $\log T_{1/2}^{exp.}$ (s) taken from⁴ and⁷⁵.

Z	N	A	$T_{1/2}^{VSS1}$	$T_{1/2}^{VSS2}$	$T_{1/2}^{PS}$	$T_{1/2}^R$	$T_{1/2}^{mR}$	$T_{1/2}^{BF}$	$T_{1/2}^{MB1}$	$T_{1/2}^{MB2}$	$T_{1/2}^{exp.}$
114	172	286	-0.21	0.19	0.08	-0.44	-0.40	-0.60	-0.60	-0.29	-0.92
114	174	288	1.17	1.51	1.42	0.90	0.93	0.63	0.55	1.08	-0.18
114	176	290	0.80	1.16	1.06	0.49	0.53	0.30	0.24	0.72	1.90
114	178	292	4.83	4.99	4.96	4.48	4.52	3.91	3.60	4.74	–
114	180	294	5.80	5.91	5.90	5.41	5.45	4.78	4.40	5.71	–
114	182	296	5.70	5.82	5.81	5.28	5.31	4.69	4.32	5.61	–
114	184	298	5.17	5.31	5.29	4.71	4.75	4.21	3.88	5.08	–
114	186	300	-1.55	-1.08	-1.22	-2.04	-2.00	-1.80	-1.72	-1.63	–
114	188	302	-0.84	-0.41	-0.53	-1.37	-1.32	-1.16	-1.13	-0.92	–
114	190	304	0.11	0.50	0.39	-0.45	-0.41	-0.31	-0.33	0.03	–
116	172	288	-1.88	-1.34	-1.50	-2.07	-2.02	-2.10	-2.07	-1.97	–
116	174	290	-0.66	-0.19	-0.33	-0.89	-0.85	-1.03	-1.07	-0.77	-2.08
116	176	292	-1.17	-0.67	-0.82	-1.44	-1.40	-1.48	-1.49	-1.28	-1.89
116	178	294	2.69	2.99	2.91	2.38	2.42	1.95	1.70	2.55	–
116	180	296	0.70	1.11	0.99	0.36	0.40	0.19	0.06	0.58	–
116	182	298	3.57	3.83	3.76	3.18	3.22	2.73	2.42	3.42	–
116	184	300	3.17	3.46	3.38	2.76	2.79	2.38	2.10	3.03	–
116	186	302	-2.84	-2.26	-2.44	-3.29	-3.25	-2.96	-2.87	-2.94	–
116	188	304	-2.22	-1.66	-1.83	-2.70	-2.65	-2.41	-2.35	-2.31	–

Table 10 – *Continued on next page*

Deformed magic numbers at $N = 178$ and $Z = 120, 124$ in superheavy region 41

Table 10 – Continued from previous page

Z	N	A	$T_{1/2}^{VSS1}$	$T_{1/2}^{VSS2}$	$T_{1/2}^{PS}$	$T_{1/2}^R$	$T_{1/2}^{mR}$	$T_{1/2}^{BF}$	$T_{1/2}^{MB1}$	$T_{1/2}^{MB2}$	$T_{1/2}^{exp.}$
116	190	306	-1.40	-0.89	-1.04	-1.92	-1.87	-1.68	-1.67	-1.50	—
118	172	290	-3.64	-2.96	-3.19	-3.78	-3.74	-3.67	-3.59	-3.73	—
118	174	292	-3.43	-2.76	-2.98	-3.61	-3.57	-3.48	-3.42	-3.52	—
118	176	294	-2.04	-1.44	-1.64	-2.26	-2.22	-2.26	-2.28	-2.15	-3.16
118	178	296	1.14	1.57	1.44	0.88	0.92	0.55	0.33	0.98	—
118	180	298	-0.96	-0.42	-0.59	-1.25	-1.21	-1.30	-1.39	-1.09	—
118	182	300	1.29	1.71	1.58	0.95	0.99	0.68	0.45	1.13	—
118	184	302	0.87	1.32	1.18	0.50	0.54	0.31	0.11	0.71	—
118	186	304	-4.58	-3.85	-4.09	-4.98	-4.93	-4.49	-4.35	-4.65	—
118	188	306	-4.04	-3.34	-3.57	-4.47	-4.43	-4.02	-3.91	-4.12	—
118	190	308	-3.34	-2.67	-2.89	-3.81	-3.76	-3.40	-3.34	-3.43	—
120	172	292	-4.29	-3.52	-3.79	-4.38	-4.34	-4.23	-4.17	-4.36	—
120	174	294	-3.86	-3.10	-3.36	-3.98	-3.94	-3.85	-3.82	-3.93	—
120	176	296	-1.98	-1.33	-1.55	-2.15	-2.11	-2.21	-2.30	-2.10	—
120	178	298	-1.35	-0.73	-0.94	-1.56	-1.52	-1.66	-1.78	-1.48	—
120	180	300	-2.98	-2.28	-2.52	-3.23	-3.18	-3.09	-3.11	-3.08	—
120	182	302	-0.99	-0.40	-0.60	-1.28	-1.23	-1.35	-1.49	-1.14	—
120	184	304	-1.39	-0.78	-0.98	-1.71	-1.67	-1.70	-1.82	-1.53	—
120	186	306	-6.16	-5.29	-5.59	-6.50	-6.45	-5.87	-5.69	-6.18	—
120	188	308	-5.65	-4.81	-5.10	-6.03	-5.98	-5.42	-5.28	-5.69	—
120	190	310	-5.05	-4.23	-4.51	-5.46	-5.41	-4.89	-4.78	-5.09	—
122	172	294	-5.31	-4.42	-4.74	-5.34	-5.29	-5.10	-5.04	-5.33	—
122	174	296	-6.13	-5.19	-5.52	-6.19	-6.14	-5.81	-5.69	-6.12	—
122	176	298	-5.05	-4.17	-4.48	-5.15	-5.10	-4.87	-4.82	-5.07	—
122	178	300	-4.26	-3.42	-3.72	-4.41	-4.36	-4.19	-4.19	-4.31	—
122	180	302	-4.84	-3.97	-4.28	-5.02	-4.97	-4.69	-4.65	-4.87	—
122	182	304	-2.99	-2.23	-2.50	-3.22	-3.17	-3.09	-3.17	-3.09	—
122	184	306	-3.32	-2.53	-2.81	-3.58	-3.53	-3.37	-3.43	-3.40	—
122	186	308	-7.57	-6.55	-6.92	-7.86	-7.80	-7.07	-6.86	-7.52	—
122	188	310	-7.14	-6.14	-6.50	-7.46	-7.40	-6.69	-6.51	-7.10	—
122	190	312	-6.57	-5.61	-5.96	-6.93	-6.88	-6.20	-6.05	-6.56	—
124	172	296	-7.74	-6.64	-7.05	-7.70	-7.65	-7.17	-7.01	-7.64	—
124	174	298	-7.88	-6.77	-7.19	-7.88	-7.83	-7.30	-7.12	-7.78	—
124	176	300	-6.21	-5.19	-5.57	-6.25	-6.20	-5.85	-5.79	-6.17	—
124	178	302	-5.82	-4.83	-5.20	-5.91	-5.86	-5.52	-5.48	-5.80	—
124	180	304	-5.96	-4.96	-5.33	-6.08	27.43	-5.63	-5.59	-5.93	—
124	182	306	-4.93	-3.99	-4.34	-5.09	-5.04	-4.75	-4.77	-4.94	—
124	184	308	-5.08	-4.13	-4.48	-5.28	-5.23	-4.88	-4.89	-5.09	—

Table 10 – Continued on next page

Table 10 – *Continued from previous page*

Z	N	A	$T_{1/2}^{VSS1}$	$T_{1/2}^{VSS2}$	$T_{1/2}^{PS}$	$T_{1/2}^R$	$T_{1/2}^{mR}$	$T_{1/2}^{BF}$	$T_{1/2}^{MB1}$	$T_{1/2}^{MB2}$	$T_{1/2}^{exp.}$
124	186	310	-9.06	-7.88	-8.32	-9.27	-9.22	-8.31	-8.06	-8.91	—
124	188	312	-8.67	-7.51	-7.95	-8.93	-8.87	-7.97	-7.75	-8.54	—
124	190	314	-8.19	-7.06	-7.48	-8.48	-8.42	-7.56	-7.37	-8.07	—
126	172	298	-8.87	-7.62	-8.10	-8.77	-8.71	-8.10	-7.92	-8.68	—
126	174	300	-8.83	-7.59	-8.06	-8.76	-8.71	-8.06	-7.89	-8.64	—
126	176	302	-8.01	-6.81	-7.27	-7.98	-7.93	-7.36	-7.24	-7.86	—
126	178	304	-7.99	-6.80	-7.25	-8.00	-7.95	-7.34	-7.22	-7.84	—
126	180	306	-7.90	-6.72	-7.17	-7.95	-7.90	-7.27	-7.15	-7.76	—
126	182	308	-7.51	-6.34	-6.79	-7.60	-7.80	-6.93	-6.84	-7.38	—
126	184	310	-7.26	-6.11	-6.55	-7.39	-7.33	-6.72	-6.64	-7.14	—
126	186	312	-11.03	-9.66	-10.18	-11.17	-11.11	-9.95	-9.63	-10.74	—
126	188	314	-10.67	-9.32	-9.84	-10.86	-10.80	-9.64	-9.35	-10.41	—
126	190	316	-10.24	-8.91	-9.42	-10.46	-10.40	-9.27	-9.00	-9.99	—
128	172	300	-9.67	-8.30	-8.83	-9.50	-9.44	-8.73	-8.55	-9.39	—
128	174	302	-9.73	-8.36	-8.90	-9.60	-9.54	-8.78	-8.60	-9.45	—
128	176	304	-9.27	-7.92	-8.45	-9.17	-9.11	-8.38	-8.24	-9.00	—
128	178	306	-9.20	-7.85	-8.38	-9.14	-9.08	-8.32	-8.18	-8.94	—
128	180	308	-9.46	-8.10	-8.63	-9.44	-9.38	-8.55	-8.39	-9.18	—
128	182	310	-9.52	-8.16	-8.69	-9.54	-9.48	-8.60	-8.43	-9.24	—
128	184	312	-9.56	-8.20	-8.73	-9.61	-9.56	-8.64	-8.47	-9.29	—
128	186	314	-13.13	-11.55	-12.17	-13.20	-13.14	-11.67	-11.27	-12.67	—
128	188	316	-12.68	-11.13	-11.74	-12.79	-12.73	-11.29	-10.92	-12.25	—
128	190	318	-12.15	-10.63	-11.23	-12.30	-12.24	-10.84	-10.50	-11.74	—
130	172	302	-10.43	-8.93	-9.53	-10.19	-10.13	-9.31	-9.14	-10.04	—
130	174	304	-10.64	-9.13	-9.74	-10.44	-10.38	-9.50	-9.31	-10.25	—
130	176	306	-10.32	-8.83	-9.42	-10.15	-10.09	-9.22	-9.05	-9.94	—
130	178	308	-10.23	-8.75	-9.34	-10.11	-10.05	-9.15	-8.99	-9.86	—
130	180	310	-10.69	-9.18	-9.78	-10.59	-10.53	-9.53	-9.34	-10.29	—
130	182	312	-10.46	-8.96	-9.56	-10.41	-10.35	-9.34	-9.17	-10.07	—
130	184	314	-10.53	-9.03	-9.63	-10.51	-10.45	-9.40	-9.22	-10.14	—
130	186	316	-13.66	-11.96	-12.64	-13.66	-13.60	-12.05	-11.66	-13.09	—
130	188	318	-13.24	-11.57	-12.24	-13.28	-13.21	-11.69	-11.33	-12.69	—
130	190	320	-11.86	-10.28	-10.91	-11.94	-11.88	-10.52	-10.26	-11.39	—

Appendix A. Comparison of alpha-decay half-lives from various equations

In this section, we compare the differences in alpha-decay half lives obtained using the various empirical equations discussed in Sec. 2.2 with respect to the average value for each nucleus. The difference in the half lives, $\log_{10} T_{1/2}$ with respect to

the average values are shown in Fig. 12, 13 and 14 for $Z = 114 - 118$, $Z = 120 - 124$ and $Z = 126 - 130$, respectively.

It easily noticeable that the VS2 parameters set consistently predict half lives which are longer than the average values for all isotopic series. In fact, VS2 half lives are the longest out of the 8 empirical equations for a given nucleus, except for some exceptions in the $Z = 126, 128$ and 130 isotopes. The PS parameters set also predicts a longer-than-average half lives, similar to the VS2, although the differences from average values decrease (i.e. closer to average value) when going towards heavier Z numbers. It is also interesting to note that the differences in half lives from average values for both VS2 and PS are rather constant for all considered isotopic series.

On the other hand, the MB1 give the most fluctuation away from the average values across a given isotopic chain. In Fig. 12, the MB1 shows half lives which are shorter than the average values for $Z = 114$ to 118 . For heavier elements shown in Fig. 13 and Fig. 14, the pattern is reversed where the MB1 results are now longer than average values. The MB2 parameters set, on the other hand, underestimate (i.e. giving shorter) the half lives as compared to the average values but with almost constant pattern across a given isotopic chain.

We now move to compare similarity in the patterns shown in Fig. 12, 13 and 14 between different parameters sets. The first group would be the original Brown parameters (denoted as B in the plots) and its modified versions MB1 and MB2. We find that the trend for B and MB1 as a function of neutron number to be rather similar for all isotopic series. On the other hand, results obtained with both B and MB1 appears to vary greatly from those using MB2.

The reason for such a huge variation in the pattern stems from the Q_α which will be addressed here. Fig. 15 shows the plot of the half lives as a function of neutron number, N , and Q_α for two isotopic samples of $Z = 114$ and 120 obtained with the SkM* parametrization. For $Z = 114$, we find that the half lives from B and MB1 to be extremely close. Results from these two sets begin to differ from the MB2 set between $N = 176$ and 184 . The Q_α within this neutron number region falls between 9.3 to 10.2 MeV (see bottom panel of Figure 15). At around this Q_α values, the MB2 half lives differs from the B and MB1 sets whereby the differences increases with decreasing Q_α . This explains the large variation in half lives between $N = 182$ and 184 for MB2 as compared to B and MB1.

Similar dependence of half lives on Q_α to explain the huge difference between B and MB1 from the MB2 is also seen for $Z = 120$. In this isotopic chain, the MB2 predicts shorter half lives as compared to B and MB1. This is attributed to the Q_α values being larger than 12 MeV. Supposed that the Q_α values for these $Z = 120$ nuclei is lower than 12 MeV, the half lives calculated using MB2 will, on the other hand, be longer as compared to those of M and MB1 sets.

The next group of semi-empirical formula which are of the same origin are the R and MR parameters sets. We found that the results obtained with these sets give rise to the same pattern with only slight variation between them. This is to be

expected since the two sets vary only by a slight change in the parameters entering the half-life equations.

To conclude this section, we also note that as one moves towards heavier elements, two distinct groups emerge. On one hand, there are the MB2, VS1, R and MR parameters sets which predict shorter half lives as compared to the average values. The other group made up of the MB1, VS2, B and PS parameters sets which predicts longer half lives.

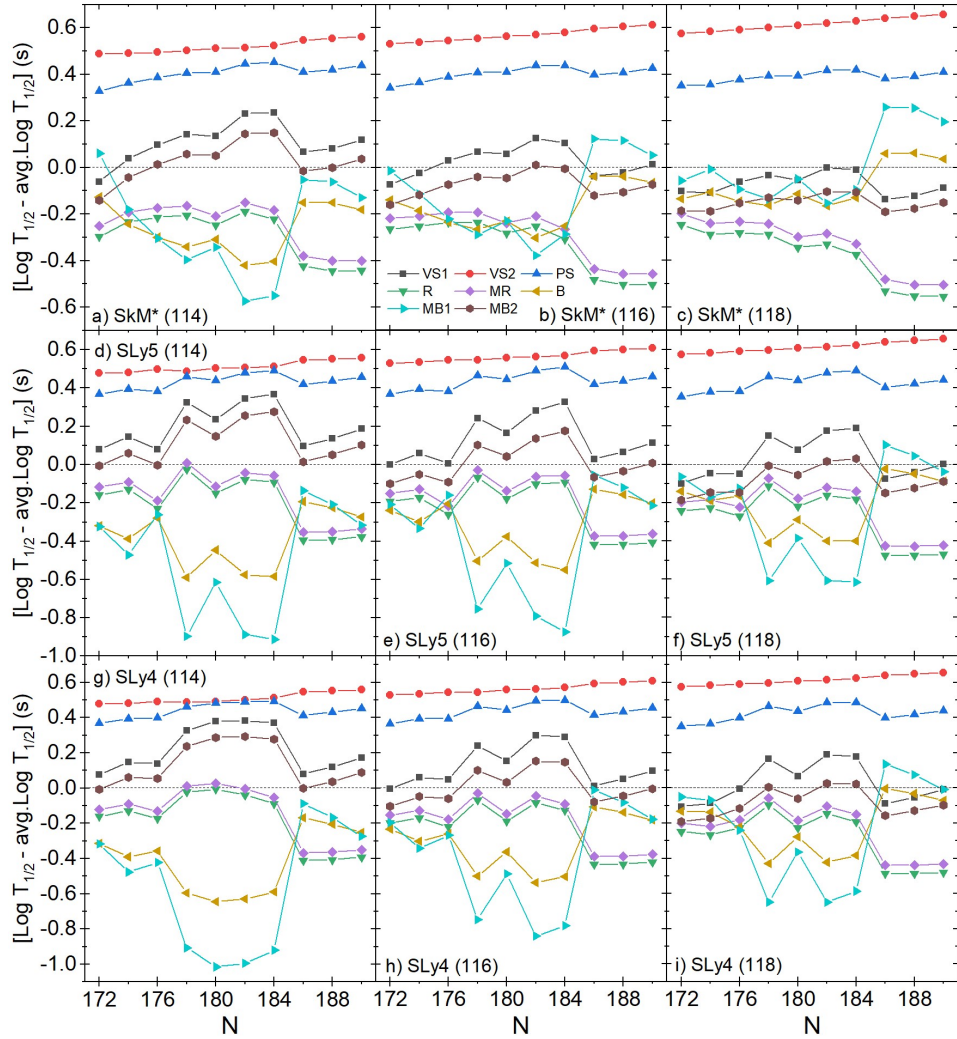


Fig. 12. Analysis of 8 different formulae for isotopes $Z = 114 - 118$ for all Skyrme paramterization (SkM*, SLy5, and SLy4).

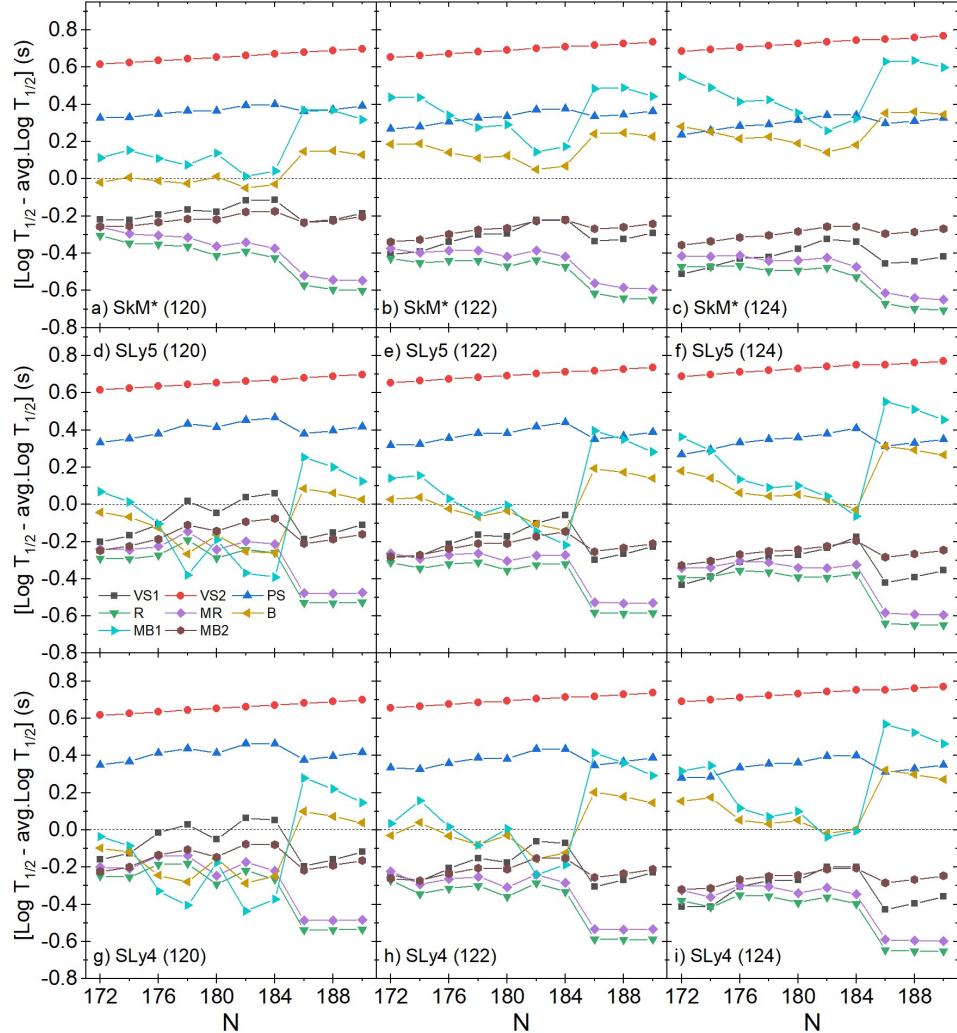


Fig. 13. Analysis of 8 different formulae for isotopes $Z = 120 - 124$ for all Skyrme parameterizations (SkM*, SLy5, and SLy4).

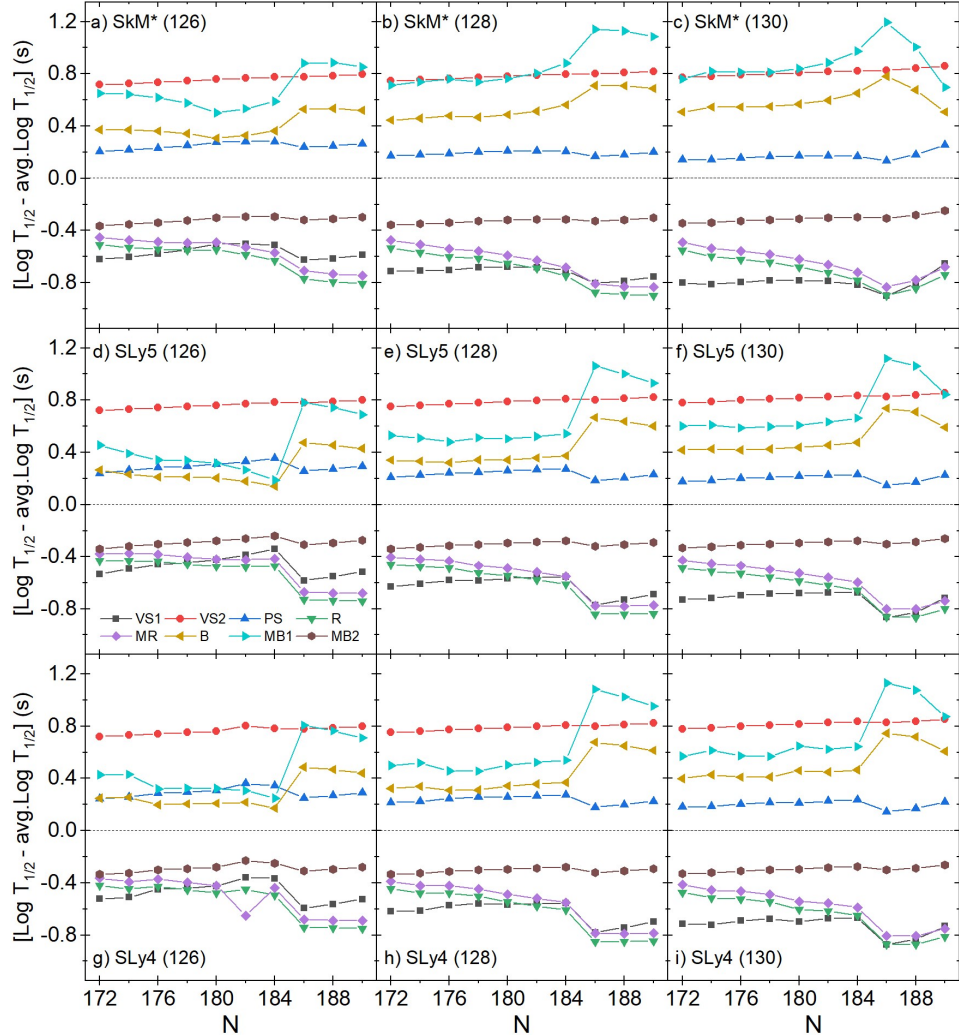
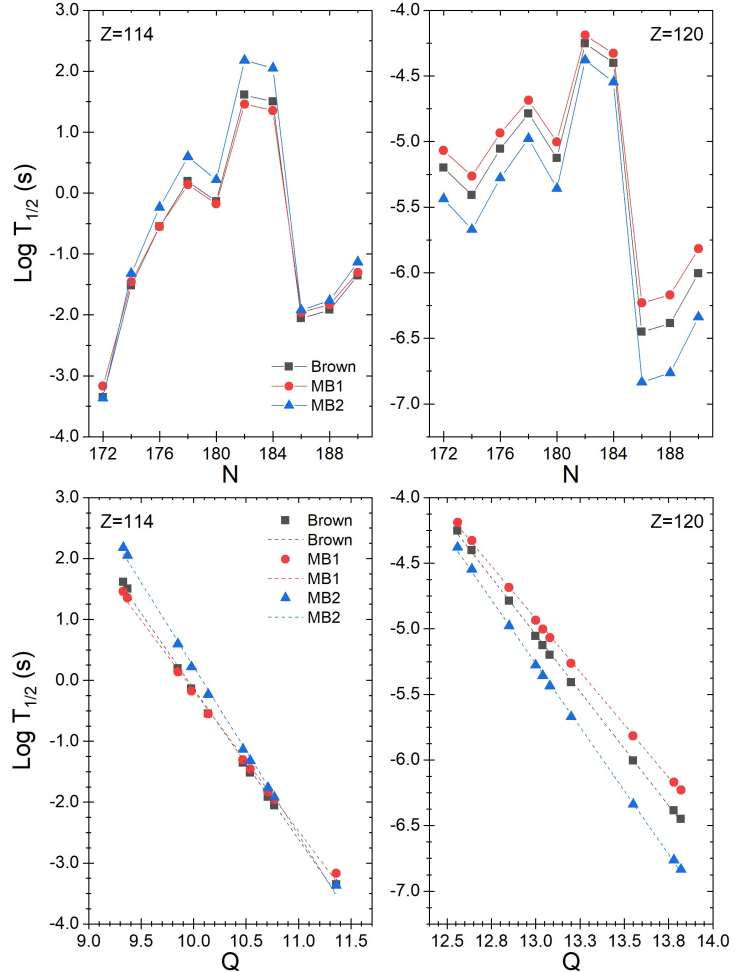


Fig. 14. Analysis of 8 different formulae for isotopes $Z = 126 - 130$ for all Skyrme parameterization (SkM*, SLy5, and SLy4).

Deformed magic numbers at $N = 178$ and $Z = 120, 124$ in superheavy region 47Fig. 15. Analysis of Brown formulae type (B, MB1, and MB2) on $Z = 114$ and $Z = 120$.

References

1. S. A. Giuliani, Z. Matheson, W. Nazarewicz, E. Olsen, P.-G. Reinhard, J. Sadhukhan, B. Schuetrumpf, N. Schunck and P. Schwerdtfeger, *Rev. Mod. Phys.* **91** (2019) 011001.
2. O. Y. Ts, V. Utyonkov, V. Lobanov Yu et al., *Phys. Rev. C* **74** (2006) 044602.
3. O. Y. Ts, A. F. Sh, C. Alexander et al., *Phys. Rev. Lett.* **109** (2012) 162501.
4. Y. T. Oganessian and V. Utyonkov, *Nucl. Phys. A* **944** (2015) 62.
5. K. Rutz, M. Bender, T. Bürenich, T. Schilling, P.-G. Reinhard, J. A. Maruhn and W. Greiner, *Phys. Rev. C* **56** (1997) 238.
6. R. K. Gupta, S. Patra and W. Greiner, *Mod. Phys. Lett. A* **12** (1997) 1727.
7. M. Bender, K. Rutz, P.-G. Reinhard, J. A. Maruhn and W. Greiner, *Phys. Rev. C* **60** (1999) 034304.
8. S. Patra, C.-L. Wu, C. Praharaj and R. K. Gupta, *Nucl. Phys. A* **651** (1999) 117.
9. A. T. Kruppa, M. Bender, W. Nazarewicz, P.-G. Reinhard, T. Vertse and S. Ćwiok, *Phys. Rev. C* **61** (2000) 034313.
10. J.-F. Berger, L. Bitaud, J. Dechargé, M. Girod and K. Dietrich, *Nucl. Phys. A* **685** (2001) 1.
11. M. Bhuyan and S. Patra, *Modern Physics Letters A* **27** (2012) 1250173.
12. W. Brodziński and J. Skalski, *Physical Review C* **88** (2013) 044307.
13. J. J. Li, W. H. Long, J. Margueron and N. Van Giai, *Physics Letters B* **732** (2014) 169.
14. Z. Shi, A. V. Afanasjev, Z. Li and J. Meng, *Physical Review C* **99** (2019) 064316.
15. J. Stone, K. Morita, P. Guichon and A. Thomas, *Phys. Rev. C* **100** (2019) 044302.
16. S. Biswal, M. A. El Sheikh, N. Biswal, N. Yusof, H. Kassim, S. Patra and M. Bhuyan, *Nuclear Physics A* **1004** (2020) 122042.
17. P. Sarriguren, *Physics Letters B* **815** (2021) 136149.
18. K. Zhang, X. He, J. Meng, C. Pan, C. Shen, C. Wang and S. Zhang, *Physical Review C* **104** (2021) L021301.
19. N. Jain, R. Kumar and M. Bhuyan, *Nucl. Phys. A* (2022) 122379.
20. P. Sarriguren, *Physical Review C* **105** (2022) 014312.
21. A. Dumitrescu and D. Delion, *Physical Review C* **107** (2023) 024302.
22. C. Xu and Z. Ren, *Phys. Rev. C* **69** (2004) 024614.
23. C. Xu and Z. Ren, *Phys. Rev. C* **73** (2006) 041301.
24. D. Ni and Z. Ren, *Nucl. Phys. A* **825** (2009) 145.
25. D. Ni and Z. Ren, *Phys. Rev. C* **80** (2009) 014314.
26. D. Ni and Z. Ren, *Phys. Rev. C* **81** (2010) 024315.
27. M. Ismail, W. Seif and A. Abdurrahman, *Phys. Rev. C* **94** (2016) 024316.
28. M. Ismail, W. Seif, A. Adel and A. Abdurrahman, *Nucl. Phys. A* **958** (2017) 202.
29. M. Ismail, A. Abdurrahman and A. Abdulghany, *Phys. At. Nucl.* **83** (2020) 691.
30. Y. Wang, Q. Gu, J. Dong and B. Peng, *International Journal of Modern Physics E* **20** (2011) 127.
31. J. Wang, H. Zhang and J. Li, *Journal of Physics G: Nuclear and Particle Physics* **40** (2013) 045103.
32. J. Cui, Y. Zhang, S. Zhang, Y. Wang et al., *Phys. Rev. C* **97** (2018) 014316.
33. K. Santhosh and B. Priyanka, *Int. J. Mod. Phys. E* **23** (2014) 1450059.
34. K. Santhosh and B. Priyanka, *Phys. Rev. C* **90** (2014) 054614.
35. H. Manjunatha, *Int. J. Mod. Phys. E* **25** (2016) 1650074.
36. K. Santhosh, B. Priyanka and C. Nithya, *Nucl. Phys. A* **955** (2016) 156.
37. H. Manjunatha, *Nucl. Phys. A* **945** (2016) 42.
38. H. Manjunatha, *Int. J. Mod. Phys. E* **25** (2016) 1650100.
39. K. Santhosh and C. Nithya, *Eur. Phys. J. A* **52** (2016) 1.

40. K. Santhosh and C. Nithya, *Phys. Rev. C* **94** (2016) 054621.
41. K. Santhosh and C. Nithya, *Eur. Phys. J. A* **53** (2017) 1.
42. K. Santhosh and C. Nithya, *At. Data Nucl. Data Tables* **119** (2018) 33.
43. K. Santhosh and C. Nithya, *At. Data Nucl. Data Tables* **121** (2018) 216.
44. K. Prathapan, K. Anjali and R. Biju, *Indian J. Phys.* (2021) 1.
45. J. Dechargé, J.-F. Berger, M. Girod and K. Dietrich, *Nuclear Physics A* **716** (2003) 55.
46. J. Dechargé, J.-F. Berger, K. Dietrich and M. Weiss, *Physics Letters B* **451** (1999) 275.
47. Y. Wang, S. Wang, Z. Hou, J. Gu et al., *Phys. Rev. C* **92** (2015) 064301.
48. Q. Mo, M. Liu and N. Wang, *Physical Review C* **90** (2014) 024320.
49. T. A. Siddiqui, A. Quddus, S. Ahmad and S. Patra, *Nuclear Physics A* **1006** (2021) 122080.
50. H.-M. Liu, J.-Y. Xu, J.-G. Deng, B. He and X.-H. Li, *International Journal of Modern Physics E* **28** (2019) 1950089.
51. L. Malov, G. Adamian, N. Antonenko and H. Lenske, *Phys. Rev. C* **104** (2021) L011304.
52. L. Malov, G. Adamian, N. Antonenko and H. Lenske, *Phys. Rev. C* **104** (2021) 064303.
53. T. Skyrme, *Nucl. Phys.* **9** (1958) 615.
54. E. Chabanat, P. Bonche, P. Haensel, J. Meyer and R. Schaeffer, *Nucl. Phys.A* **635** (1998) 231.
55. A. Pastore, D. Davesne, K. Bennaceur, J. Meyer and V. Hellemans, *Phys. Scr.* **2013** (2013) 014014.
56. S. Ćwiok, W. Nazarewicz and P.-H. Heenen, *Phys. Rev. Lett.* **83** (1999) 1108.
57. C. Peng and Z.-Q. Feng, *Communications in Theoretical Physics* **74** (2022) 055302.
58. J. C. Slater, *Phys. Rev.* **81** (Feb 1951) 385.
59. H. Flocard, P. Quentin, A. Kerman and D. Vautherin, *Nuclear Physics A* **203** (1973) 433.
60. V. Viola Jr and G. Seaborg, *J. inorg. nucl.* **28** (1966) 741.
61. A. Sobczewski, Z. Patyk and S. Ćwiok, *Phys. Lett. B* **224** (1989) 1.
62. A. Parkhomenko and A. Sobczewski, *Acta Phys. Pol. B* **36** (2005) 3095.
63. A. Sobczewski and K. Pomorski, *Progress in Particle and Nuclear Physics* **58** (2007) 292.
64. G. Royer, *J. Phys. G: Nucl. Part. Phys.* **26** (2000) 1149.
65. G. Royer, *Nucl. Phys. A* **848** (2010) 279.
66. D. T. Akrawy, H. Hassanabadi, S. Hosseini and K. Santhosh, *Nucl. Phys. A* **971** (2018) 130.
67. B. A. Brown, *Phys. Rev. C* **46** (1992) 811.
68. A. Budaca, R. Budaca and I. Silisteanu, *Nucl. Phys. A* **951** (2016) 60.
69. K.-W. Kelvin-Lee, M.-H. Koh, L. Bonneau et al., *Phys. Rev. C* **103** (2021) 064315.
70. J. Maruhn, P. Reinhard, P. Stevenson, J. R. Stone and M. Strayer, *Physical Review C—Nuclear Physics* **71** (2005) 064328.
71. A. Karim and S. Ahmad, *Chin. J. Phys.* **59** (2019) 606.
72. M.-H. Koh and P. Quentin, *Phys. Rev. C* **110** (2024) 024311.
73. S. Ćwiok, J. Dobaczewski, P.-H. Heenen, P. Magierski and W. Nazarewicz, *Nucl. Phys. A* **611** (1996) 211.
74. S. Ćwiok, P.-H. Heenen and W. Nazarewicz, *Nature* **433** (2005) 705.
75. NNDC Database, <https://www.nndc.bnl.gov/nudat3/>.
76. N. Wang, M. Liu, X. Wu and J. Meng, *Phys. Rev. C* **93** (2016) 014302.
77. O. Ghodsi and M. Hassanzad, *Phys. Rev. C* **101** (2020) 034606.